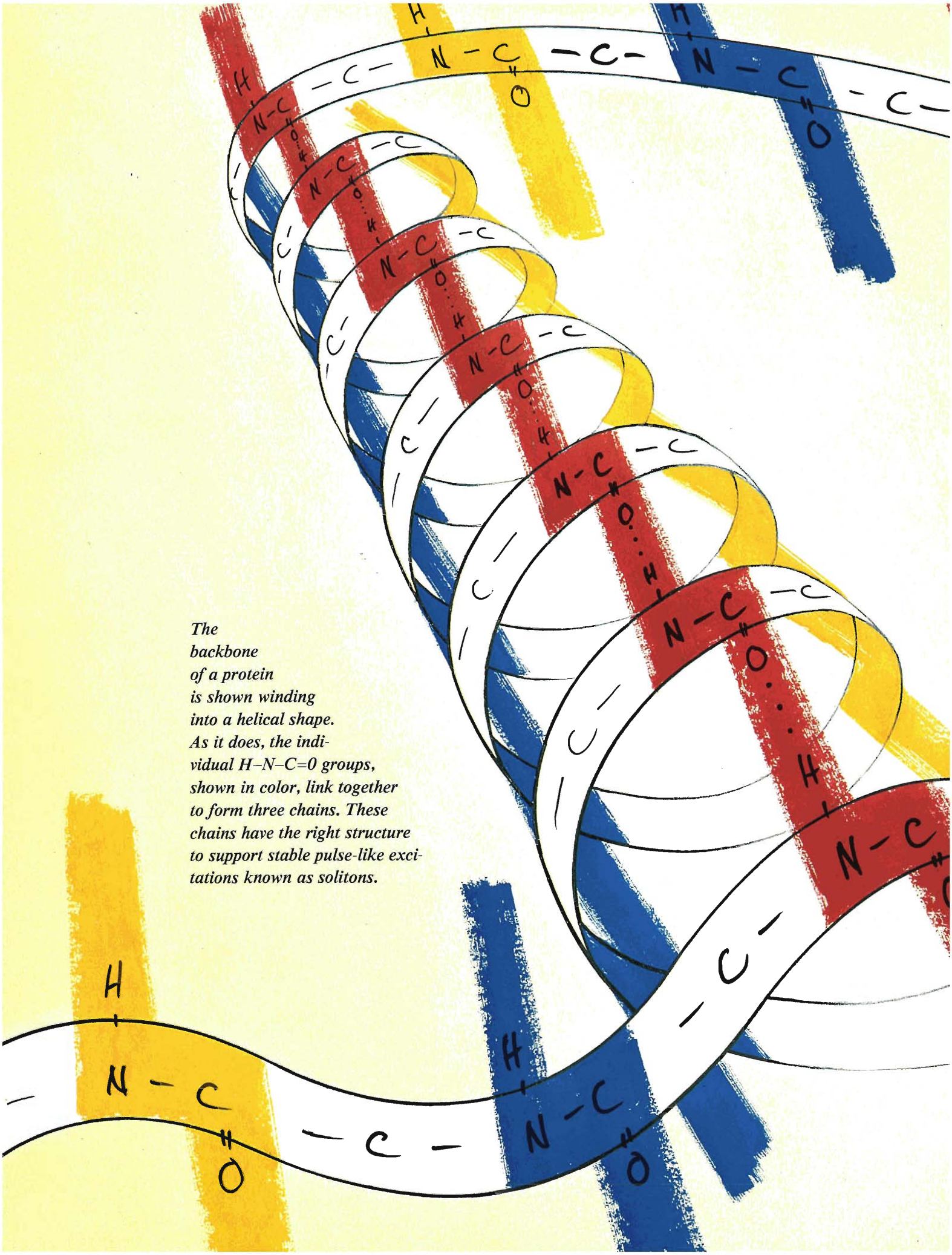

The backbone of a protein is shown winding into a helical shape. As it does, the individual H–N–C=0 groups, shown in color, link together to form three chains. These chains have the right structure to support stable pulse-like excitations known as solitons.

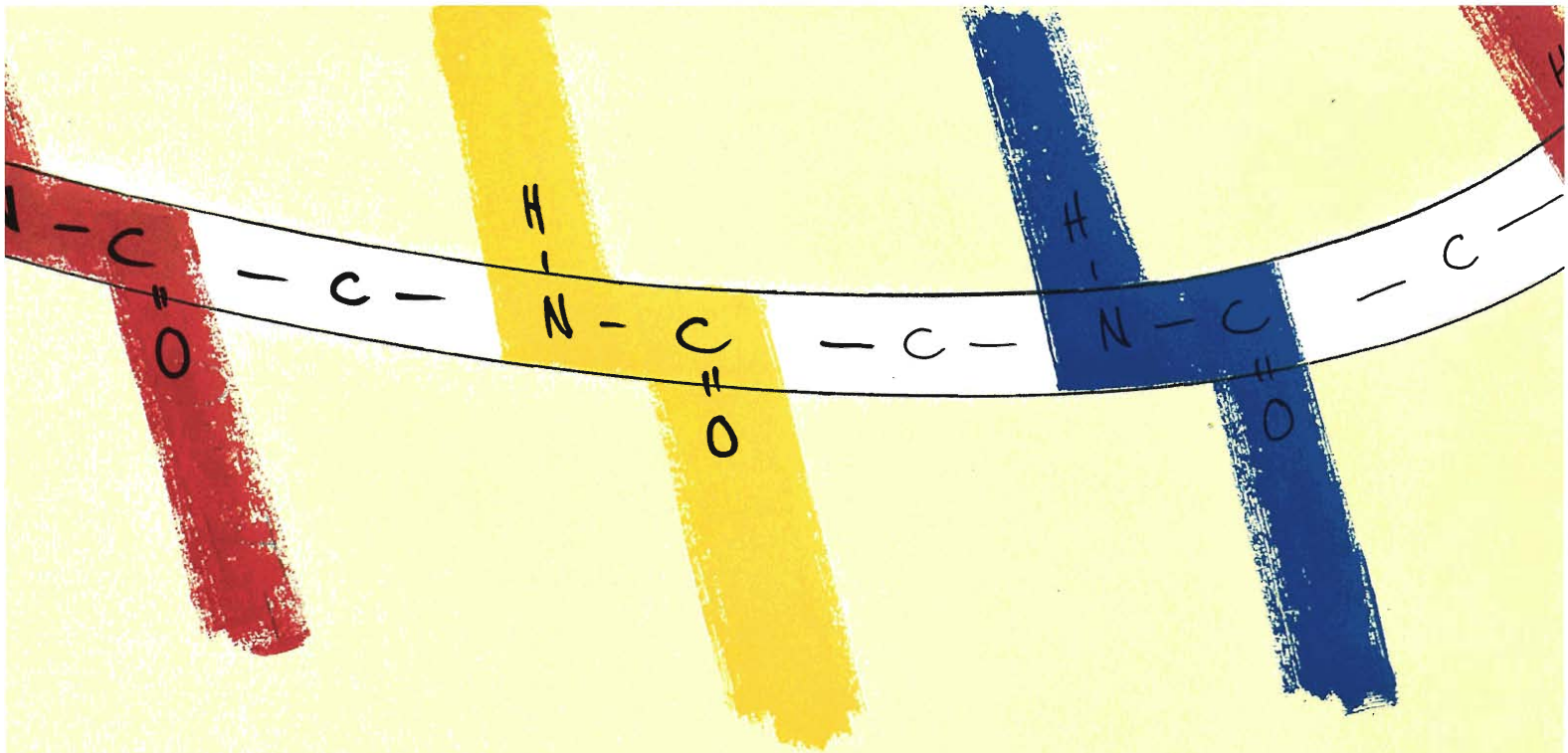

Solitons in Biology

by Peter S. Lomdahl, Scott P. Layne, and Irving J. Bigio

In 1973 scientists gathered at the New York Academy of Sciences to discuss an unanswered question in bioenergetics: How is chemical energy transduced and transported in biological systems? In the same year a Soviet solid-state physicist proposed a dynamic answer that was totally novel to the world of biology. Exploiting the regularity in the structure of α-helical proteins, he showed that simplified models of these proteins could self-focus, or trap, energy in stable, pulse-like waves known as solitons. If self-focusing is indeed a biological reality, it may account for many aspects of protein behavior, including the efficient transport of energy. This possibility is being studied at Los Alamos through analytical, numerical, and experimental techniques.

It is widely accepted that proteins are the principal workhorses of the cell. They are the major organizers and manipulators of biological energy and the enzymes that catalyze and maintain the life process. They are responsible for the active transport of ions into and out of the cell and for cellular and intracellular movement. Of course other macromolecules, such as DNA, polysaccharides, and lipids, have an energetic dimension, but their operation is always closely tied to that of proteins. Therefore the discipline of bioenergetics, which is the study of how cells generate and transfer their energy supply, is primarily the investigation of how proteins work. From decades of chemical analysis and x-ray crystallography and from more recent advances in spectroscopy, we know the composition and three-dimensional conformation of about two hundred proteins. Despite this extensive structural knowledge, however, there is no generally accepted model of how proteins operate dynamically. Presently, it is fair to say that the "nuts and bolts" functioning of proteins remains an outstanding question in bioenergetics.

The energy supply for most protein activities is provided by the hydrolysis of ATP (adenosine triphosphate). An ATP molecule binds to a specific site on the protein, reacts with water, and under normal physiological conditions releases 0.49 electron volt (eV) of free energy. This is about twenty times greater than the average energy available from the thermal background at 300 kelvins. The question for bioenergetics is what happens to this energy? How does it perform useful work? Is the energy used through a nonequilibrium process, or does the energy first thermalize and then work through an equilibrium process? Molecular dynamics calculations, based on ball-and-spring models of proteins, show that heat from a thermal bath induces a variety of motions in proteins. These equilibrium calculations show motions ranging from localized, high-frequency vibrations of individual bonds to collective, low-frequency motions of the entire protein. One may question, however, whether such equilibrium dynamics could account for the efficient transport and use of energy over the characteristic lengths of proteins, which range from tens to hundreds of angstroms.

An alternative hypothesis is that the energy of ATP hydrolysis is converted through resonant coupling to a particular vibrational excitation within the protein. This coupling might proceed through an intermediate vibrational excitation of water. Figure 1 shows a likely recipient in such a resonant exchange, the amide-I vibration. This vibration is primarily a stretching and contraction of the carbon-oxygen double bonds in the peptide groups of the protein (see "The Structure of Proteins"). The energy of the amide-I vibration is about 0.21 eV, which corresponds to about 1660 reciprocal centimeters (cm^{-1}).* This energy is a little less than half the energy of ATP hydrolysis and is almost equal to the energy of the H–O–H bending mode of water at about 1646 cm^{-1}. The amide-I vibration is a prominent feature in the infrared absorption and Raman spectra of

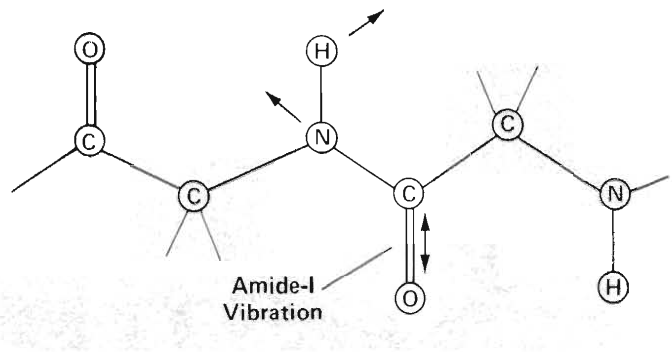

Fig. 1. Peptide group showing amide-I resonance. The amide-I resonance, which is intrinsic to every peptide bond of every protein, is one of the strongest and most characteristic spectral features of a protein. Its energy is nearly invariant from one protein conformation to another (1645 to 1660 cm^{-1} for an α helix, 1665 to 1680 cm^{-1} for a β sheet, and 1660 to 1665 cm^{-1} for a random coil). The major contribution to the amide-I resonance comes from the stretching vibration of the C=O bond, although relatively small contributions come from both the C–N in-plane stretching and N–H in-plane bending vibrations.

proteins. Moreover, its energy remains almost constant from one protein conformation to another, indicating that it is rather isolated from other degrees of freedom. All these factors lead to the conjecture that the energy released by ATP hydrolysis might stay localized and stored in the amide-I vibration.

When a similar idea was discussed at the 1973 meeting of the New York Academy of Sciences, the objection was raised that the lifetimes of typical vibrational excitations in complex biological molecules are too short (10^{-12} second) for them to be important in the storage and transfer of biological energy. In particular, peptide groups have large electric dipole moments; therefore, dipole-dipole interactions among peptide groups would cause the amide-I vibrational energy to spread to neighboring peptide groups. Thus the energy would not remain localized but instead would disperse throughout the protein and be lost as a source for biological processes.

The Soviet physicist A. S. Davydov countered this objection with an argument from nonlinear physics. He suggested that the energy of ATP hydrolysis can be stored in the amide-I vibration through a nonlinear interaction that self-focuses, or traps, the energy in a soliton

**In spectroscopy one often uses the wave number $1/\lambda = \omega/2\pi c = E/hc$, instead of the energy E or frequency ω, to characterize vibrational states since the typical numbers are more palatable.*

Structure of Proteins

Proteins are constructed from individual building blocks called amino acids. In all about twenty different amino acids are commonly found in proteins, and about five others are found rarely. Each amino acid has an amino group (NH_2), a carboxyl group (COOH), and a side group, or radical (R), attached to the alpha carbon atom. It is the radical that distinguishes one amino acid from another.

Amino Acid

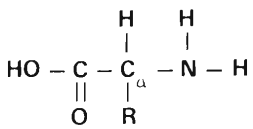

R = Side Chain on Alpha Carbon

Amino acids polymerize to form long chains of residues that constitute a protein. When two amino acids join together, they liberate one molecule of water and form a peptide bond as shown below. Thus the protein is a long polypeptide chain.

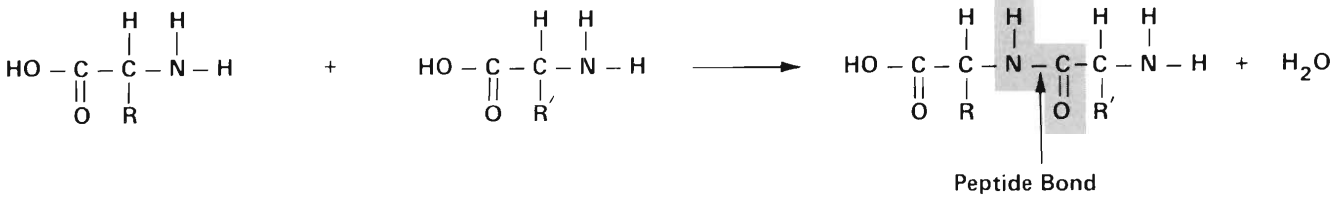

Once a protein chain forms, it can fold into a variety of complex three-dimensional conformations. Among the possible conformations usually only one exhibits biological activity. This "native" conformation generally minimizes the free energy of the protein and is therefore the most stable. Many factors contribute to this stability including hydrogen bonding, disulfide bonding, Van der Waals forces, and solvent interactions.

Three common structural motifs recur over and over again in proteins: the α helix, the β sheet, and the globular conformation. In the α helix the chain is tightly coiled about its longitudinal axis. In the zigzag β sheet the chain can be visualized as pleated strands of protein. In the globular conformation, which is the most complex, the chain is irregularly and tightly folded into a compact, nearly spherical shape. Short stretches of the chain are often constructed from α helices or β sheets.

Many large proteins consist of smaller protein subunits that interlock into one macromolecule. Such complex structures operate as coordinated factories in which each subunit contributes a specialized function to the macromolecular protein. ■

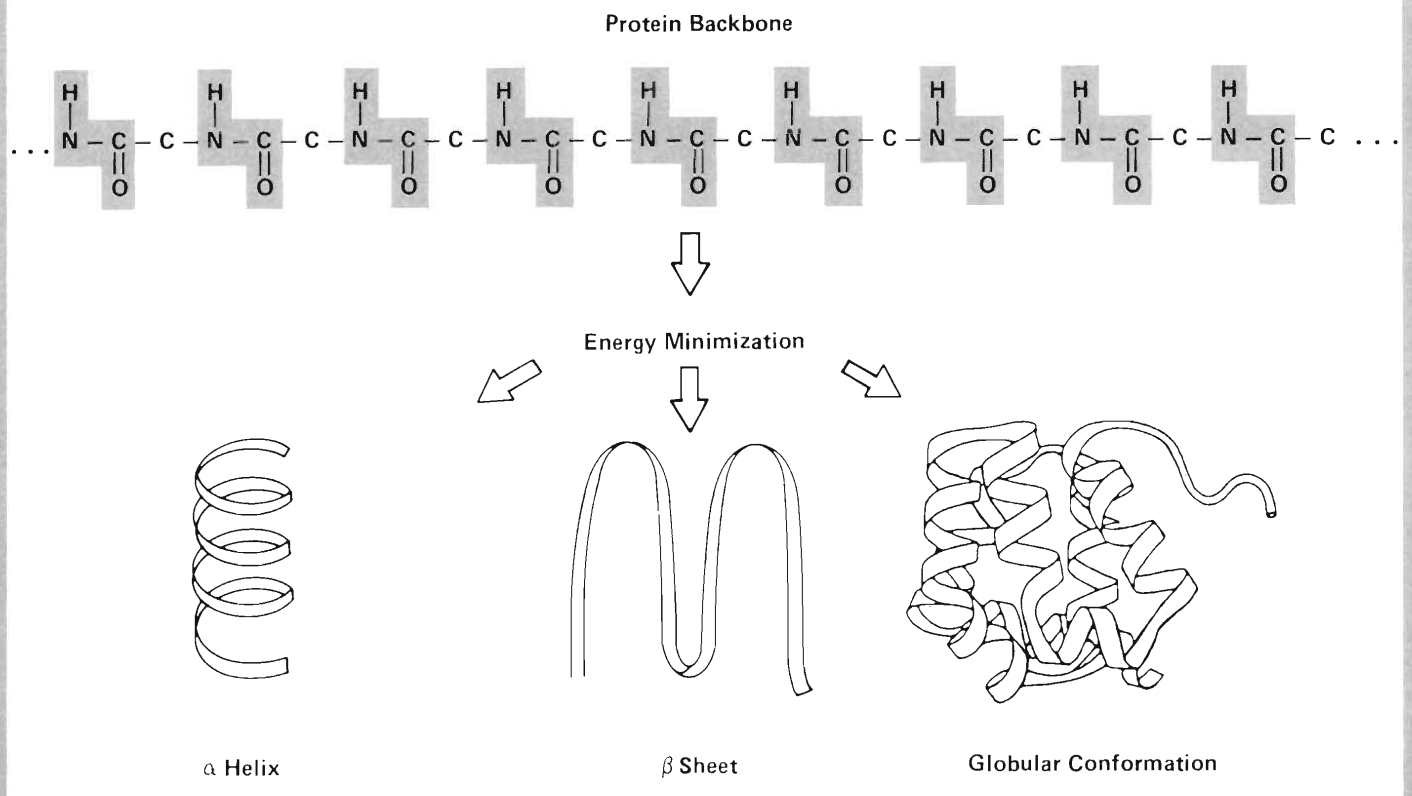

(see "What Is a Soliton?"). The soliton results from a nonlinear coupling between the vibrational excitation and a deformation in the protein structure caused by the presence of the excitation. The excitation and the deformation balance each other, and the resulting excitation moves through the protein uninhibited, much the way electrons move in the superconducting state of a metal.

Davydov worked out these ideas for one particular protein conformation, the α helix pictured at the beginning of this article. He introduced a simple mathematical model to show how solitons could travel along the three spines, or hydrogen-bonded chains, of the protein.

Davydov first applied this idea to the problem of muscle contraction. He proposed that myosin, a major contractile protein in striated muscle that has an α-helical tail approximately 1500 angstroms long, propagates a soliton that squeezes and pulls on the actin filaments around it. This action serves to slide the actin and myosin filaments together and thereby results in muscle contraction. In addition, Davydov and his coworkers have considered the idea that α-helical proteins may facilitate electron transport through a soliton mechanism. In this case an extra electron causes a lattice distortion in the protein that stabilizes the electron's motion. Thus it may be reasonable to consider charge transfer across membranes, energy coupling across membranes, and energy transport along filamentous cytoskeletal proteins in terms of a soliton mechanism, since the proteins that carry out these functions contain structural units with significant α-helical character.

The soliton model is one of several concepts for protein dynamics that should attract the careful attention of biologists. Clearly, it cannot explain every aspect of protein dynamics, but it is motivating exciting questions and new experiments. In the following sections we will describe Davydov's concept in the context of the α helix and expand it to a crystalline polymer called acetanilide, which was observed by G. Careri to have an anomalous spectral line near the amide-I band that might be due to a soliton. We will discuss experimental techniques for verifying the existence of solitons in α-helical proteins and acetanilide and consider the concept of self-focusing in globular proteins. (A further application of the soliton model is discussed in "A Possible Mechanism for General Anesthesia.")

Before discussing details of the soliton model, we will try to make the relevant biological context more vivid to the reader by presenting three specific examples where soliton-like dynamics may well be operating.

Three Sites of Action at a Distance

Alpha-helical structure is quite common in proteins, and in particular it is present where energy appears to be transported from one end of a protein to the other or where two processes appear to be coupled by a protein.

Mitochondria. Mitochondria are the energy-generating stations for living cells. These organelles, which may have evolved from separate organisms that were later incorporated into the cell, occupy approximately 20 percent of the total cellular volume. Within these organelles has developed a very specialized protein unit specifically designed to synthesize ATP. It is called the tripartite repeating unit (Fig. 2). Numerous copies of this unit make up the flexible inner membrane of a mitochondrion. As shown in Fig. 2, each time three ATP molecules are synthesized in the head of the F_0–F_1 protein, a pair of electrons (which are donated by the Krebs cycle via the intermediate NADH) circulates among the membrane-bound electron-transport proteins (labeled I, II, III, and IV). The electrons ultimately combine with oxygen and protons to produce water. The movement of these electrons back and forth across the inner membrane, in turn, creates a proton gradient across the membrane that drives the synthesis of ATP in the head of the F_0–F_1 protein. At present, the nature of the driving mechanism is an open question. How do the cytochrome proteins in subunits I, II, III, and IV facilitate electron and proton transport across the thickness (about 60 angstroms) of the inner mitochondrial membrane and at the same time couple ion transport to ATP synthesis? (Semiclassical theories account for electron tunneling between the donor and acceptor heme groups that are attached to the cytochrome proteins and have thus explained oxidation-reduction rates in cytochromes. These theories, however, have not connected electron tunneling to ATP synthesis.)

The dominant configuration of the cytochromes is α-helical, and these proteins span the inner membrane. Given these facts we may ask whether a soliton-like mechanism in these proteins may have anything to do with the stabilization of electron transport and its connection to ATP synthesis.

A related question concerns the contracted configuration of a mitochondrion during ATP synthesis. When a mitochondrion is inactive, its inner membrane is relaxed and spread out, but when active, its inner membrane abruptly contracts into a more wrinkled and twisted appearance (Fig. 3). This brings the myriad tripartite repeating units in the inner membrane into closer apposition with one another. Apparently this aggregation of transmembrane proteins is a prerequisite for ATP synthesis. Whether or not this aggregation induces a change in the conformation of the individual transmembrane proteins is not clear. However, if a soliton-like mechanism were operating during ATP synthesis, it could well be affected by such changes in protein conformation.

Cytoskeleton. The cytoskeleton is a framework of interconnected proteins that literally fills and bridges the inside of a cell (Fig. 4). It provides an internal structure on which the "bag" of the cell rests

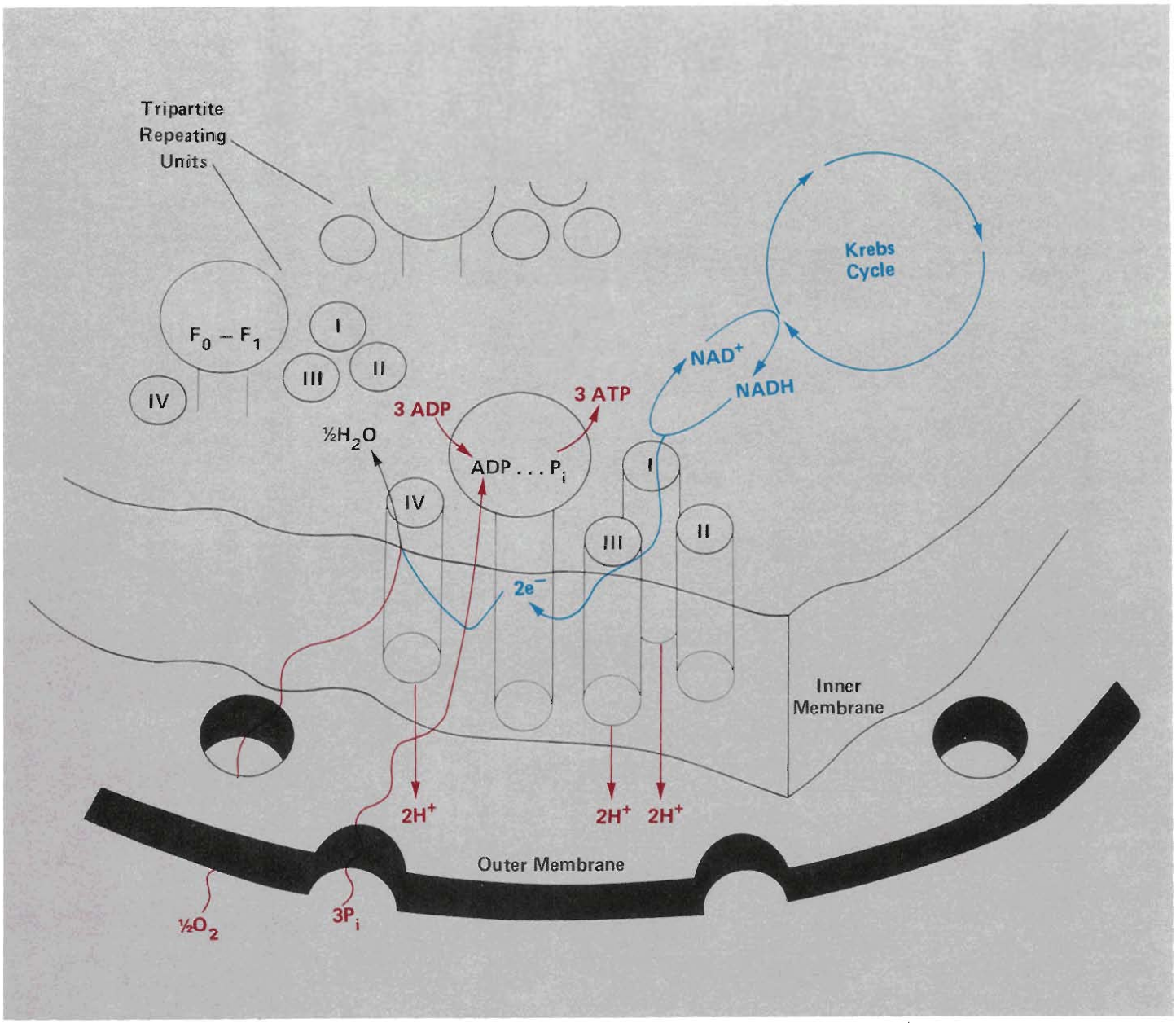

Fig. 2. Cross section of the mitochondrial membrane showing ATP synthesis (red) and electron transport (blue). These two processes both take place in the tripartite repeating units of the flexible inner membrane, and they appear to be coupled. For every three ATP molecules synthesized in the head of the mushroom-shaped central protein F_0–F_1, a pair of electrons circulates through three of the four membrane-bound protein subunits (I, III, and IV) and combines with oxygen and protons to form water. The electron pair is donated by the Krebs cycle through the intermediate NADH. A proton gradient across the inner mitochondrial membrane couples ATP synthesis to the electron transport, or respiratory, chain, but it is not clear how electron transport is related to proton pumping.

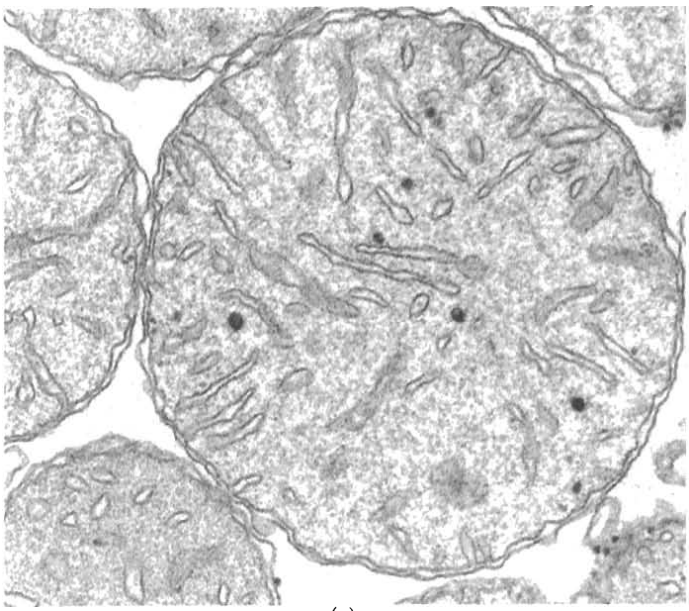

(a)

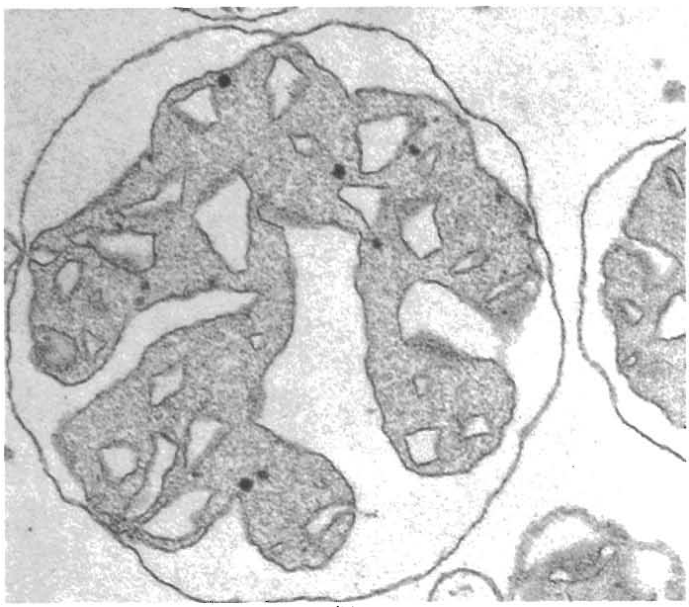

(b)

Fig. 3. Electron micrograph of isolated rat-liver mitochondria fixed in the (a) inactive and (b) active conformations. When a mitochondrion is actively synthesizing ATP, its flexible inner membrane contracts around the inner contents of the mitochondrion (darker area) and brings the tripartite repeating units of the inner membrane in closer apposition. (These micrographs, courtesy of C. Hackenbrock, appear in Mitochondria *by Alexander Tzagoloff (Plenum Press, 1982).)*

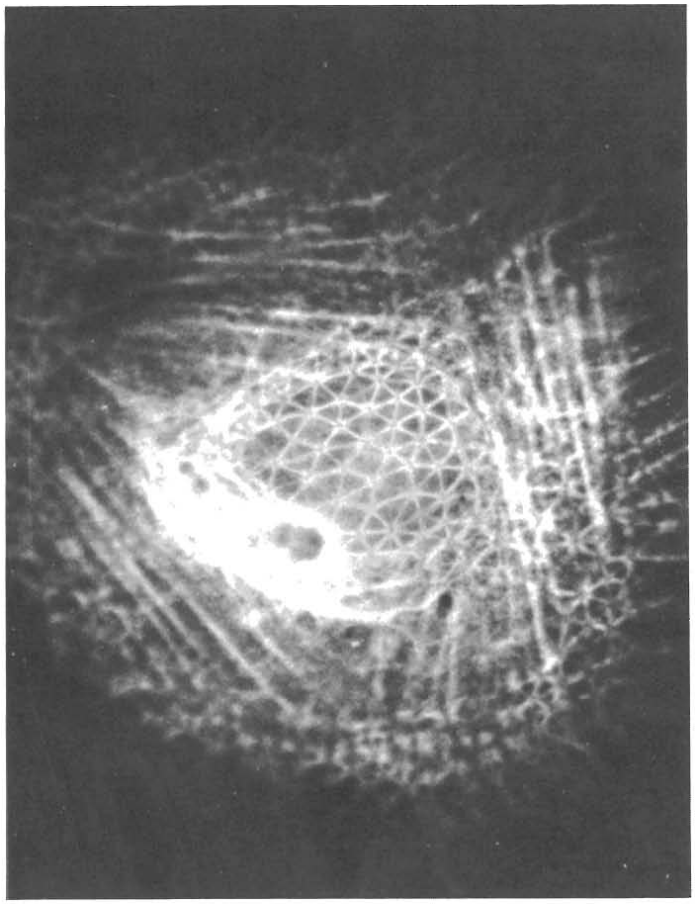

Fig. 4. Immunofluorescence micrograph showing a portion of the cytoskeleton from a cultured rat-embryo cell at a magnification of 10,000. The micrograph was prepared with anti-tropomyosin. The geodesic network of bundles visible in the micrograph forms around the cell's nucleus as the cell changes from a motile to a spread-out, immotile state. (Micrograph courtesy of E. Lazarides.)

itself and on which the cell moves, divides, and changes its outer shape. More recent discoveries suggest that it may be an internal "telegraph network" that allows for intracellular communication or an energetic "conduit" on which the soluble enzymes of the cytosol attach and coordinate their metabolic activities. In any case the cytoskeleton is constantly remodeling itself to meet the demands of the cell. This requires the expenditure of ATP, which in turn appears to be under the fine control of Ca^{2+} concentrations within the cellular juice.

In the proteins of the cytoskeleton, the α helix is a common structural motif. At least three contractile proteins are highly α helical: spectrin, tropomyosin, and myosin. There is also an extensive network of intermediate filamentous proteins within the cytoskeleton that has a predominantly helical character. Cytoskeletal proteins tend to be much longer (300-1500 angstroms) than membrance proteins, and they also tend to form very stable coiled-coil structures, which are capable of polymerizing in a head-to-tail configuration to create exceptionally long α-helical networks within the cytosol. Therefore, it is again reasonable to consider that soliton-like dynamics may be helpful for understanding energy transfer in these longer proteins, where equilibrium models of protein behavior fail to account for translational dynamics.

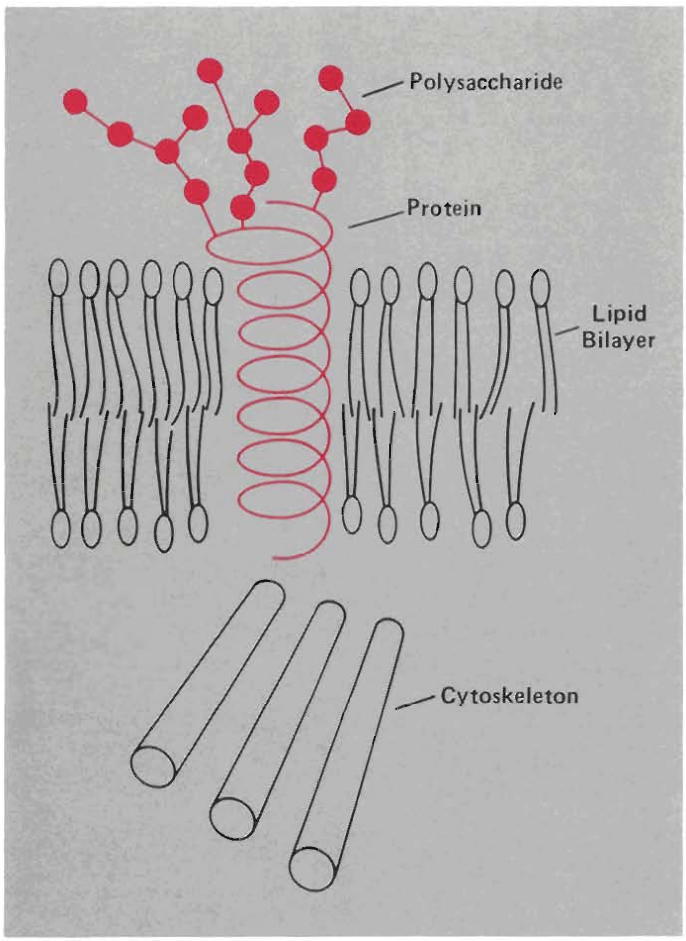

Fig. 5. Glycoproteins (red) embedded in a cell membrane physically connect the inside and the outside of the cell. The polysaccharide portion of the glycoprotein is on the cell surface, and the protein portion juts through the lipid bilayer to form the membrane channels. Some glycoproteins are closely associated with microfilaments and microtubules in the cytoskeleton.

Glycoproteins. Glycoproteins are combinations of sugars and proteins that are covalently bonded together. In the lipid bilayer, or outer membrane, of a cell are numerous glycoproteins, which vary markedly in size and chemical composition (Fig. 5). Many of these macromolecules span the entire thickness of the lipid bilayer; that is, they physically connect the inside and the outside of the cell. As a glycoprotein floats in the lipid bilayer, its polysaccharide portion is in the aqueous phase surrounding the cell, while most of its protein portion is in the lipid phase of the membrane. These transmembranous glycoproteins are crucial to the livelihood of the cell. They are implicated in cellular adhesion, cellular migration, cellular identity, intercellular communication, and transmembrane signaling. They allow a ready pathway over which signals that originate on the cellular exterior (through the binding of a hormone, neurotransmitter, or immunoglobulin) are conveyed directly to the cellular interior.

Much of the protein fraction of a glycoprotein is in the α-helical conformation. Thus information about events on the outside of a cell may be conveyed through a helical channel across the thickness of the lipid bilayer (about 60 angstroms). Therefore, nonlinear dynamics may again provide a key for understanding the mechanisms by which chemical "whispers" are detected and processed on the membrane surface.

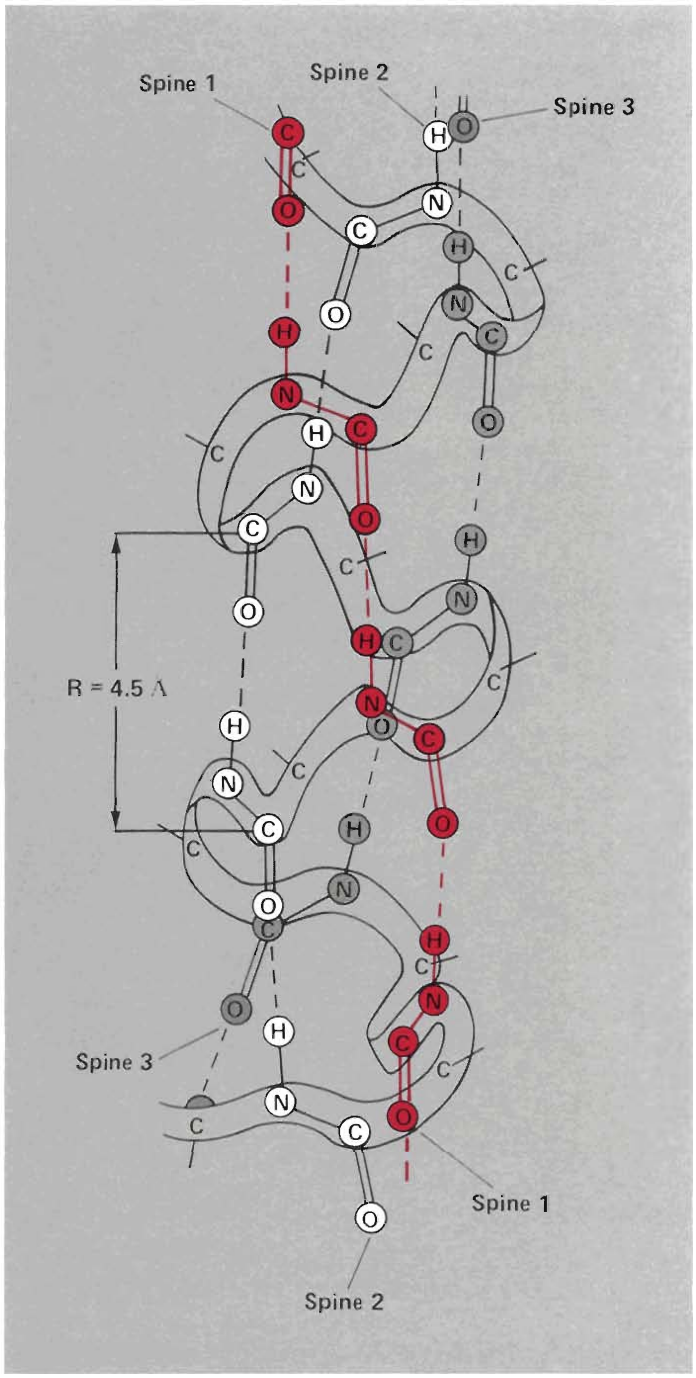

Fig. 6. Portion of an α-helical protein showing the three spines of hydrogen-bonded peptide groups. The dipole moment of each peptide group is approximately colinear with the adjacent hydrogen bond.

Solitons on the α Helix

Alpha-helical proteins, which are implicated in so many ways in energy transport and energy coupling, are the context for Davydov's theory. As the name implies, the conformation of these proteins is a helix formed by the twisting of the protein backbone. In addition, hydrogen bonds link the peptide groups together to form three spines that span the length of the helix and stabilize it. (The reader might like to make a model of the protein backbone like the one pictured in the opening figure. To form the helix, wind the backbone into a right hand spiral and attach the hydrogen of the first peptide group to the oxygen of the fourth group, the hydrogen of the second peptide group to the oxygen of the fifth, and so on. Note the formation of three spines of hydrogen-bonded peptide groups. The first spine consists of the first, fourth, seventh, tenth, etc., peptide groups. The second and third spines form similarly.) The spines of an α-helical protein are not exactly linear or parallel to the axis of the helix (Fig. 6), but nevertheless the electric dipole moments $\vec{d}$ of the amide-I vibrations are essentially in the same direction as the hydrogen bonds that define the spine. This fact, as we will see, leads to cooperative behavior along each chain of hydrogen-bonded peptide groups.

Consider a single linear chain of hydrogen-bonded peptide groups. Figure 7 shows three interactions that occur when an amide-I vibration in a particular peptide group is excited, say, by the hydrolysis of ATP. First (Fig. 7a), there will be resonant interactions with neighboring peptide groups due to electromagnetic dipole-dipole interactions, much like the interaction between transmitting and receiving antennae of a radio system. This interaction alone would lead to dispersion of amide-I energy. Second (Fig. 7b), due to changes in static forces (hydrogen bonds, Van der Waals forces, etc.), the

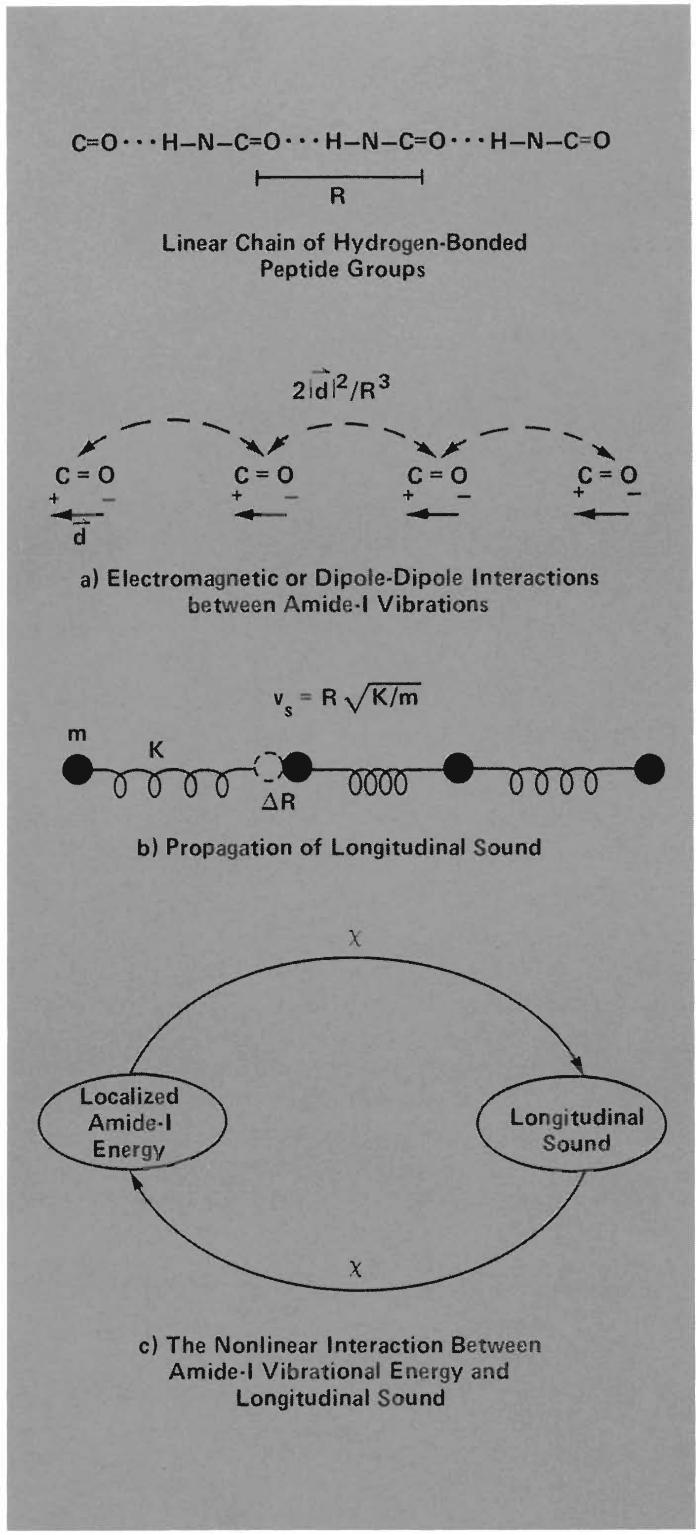

Fig. 7. Linear chain of hydrogen-bonded peptide groups showing the three interactions that combine to trap amide-I vibrational energy in a stable solitary wave, or soliton. Peptide groups with electric dipole moments $\vec{d}$ ***are separated by a distance*** R ***from each other. (a) The dipole-dipole interaction energy between neighbors on the chain is equal to*** $2|\vec{d}|^2/R^3$. ***(b) A peptide group of mass m displaced*** $\triangle R$ ***from its equilibrium position sets up a longitudinal sound wave along the chain. The wave travels at velocity*** $v_s = R(K/m)^{1/2}$, ***where*** K ***is the strength of the weak spring that represents the hydrogen bond between peptide groups. (c) The nonlinear interaction between amide-I vibrational energy and longitudinal sound is represented by a feedback loop in which one interaction reacts back on the other and vice versa. The strength of the interaction is proportional to*** χ^2 ***and inversely proportional to*** K.

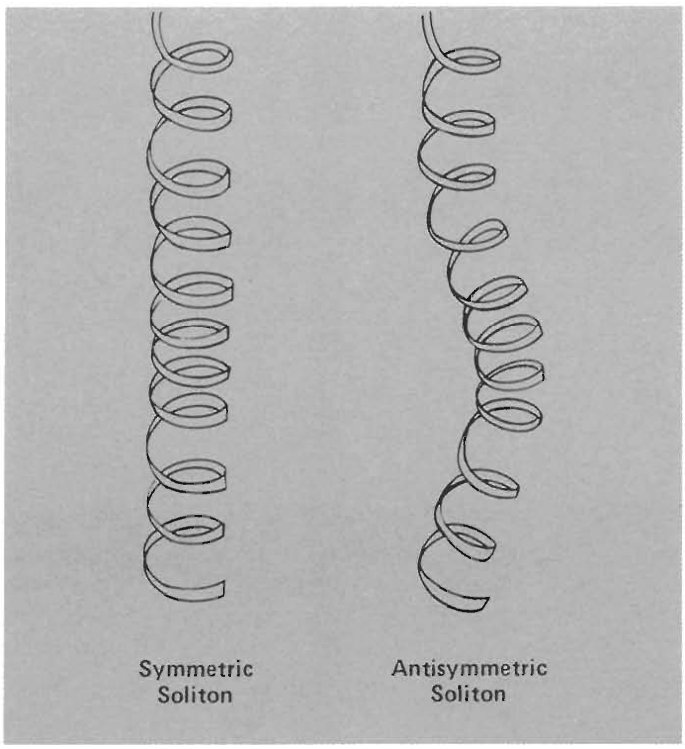

Fig. 8. Two types of solitons can form on the α helix: (1) a symmetric soliton in which amide-I vibrational energy is shared equally among the three spines, and (2) an antisymmetric soliton in which amide-I energy is shared unequally. The soliton is localized over about four turns of the helix. The symmetric soliton causes compression in the longitudinal direction, and the antisymmetric soliton causes bending of the helix.

excited peptide group will tend to move from its equilibrium position, causing a local deformation of the hydrogen bond in the region of excitation. In α-helical proteins the largest displacement will also be along the hydrogen bonds because hydrogen bonds are weaker than the covalent bonds along the helix. Since the hydrogen bond behaves like a weak spring, this movement of the peptide group away from equilibrium will set up a longitudinal sound wave, or phonon, along the chain as the peptide groups oscillate about their equilibrium positions.

These two dynamical effects are displayed in Fig. 7 as if they were uncoupled; that is, dispersion of amide-I bond energy (Fig. 7a) is independent of the propagation of longitudinal sound waves (Fig. 7b). Davydov, however, pointed out that the two effects are coupled by a *nonlinear* interaction that arises from the change in amide-I vibrational energy E caused by a change in the distance R between peptide groups along the chain (hydrogen-bond stretching). The strength of this coupling is proportional to the nonlinear parameter

$$\chi \equiv \frac{dE}{dR} ,$$

which can be expressed in units of joules per meter, or newtons. The effect of this nonlinear coupling is displayed graphically in Fig. 7c. Localized amide-I vibrational energy acts (through χ) as a source of longitudinal sound, and this longitudinal sound reacts (again through χ) as a potential well that traps the amide-I vibrational energy and prevents its dispersion. Coupled together, the localized amide-I vibrational energy and the longitudinal deformation can travel along the chain as a soliton with no energy loss.

As shown in the next section, this soliton is described by the nonlinear Schrödinger equation. Figure 7c shows that the strength of the nonlinear effect is proportional to χ^2. It is also inversely proportional to K, the spring constant of the hydrogen bonds connecting the peptide groups. If the linear chain were absolutely rigid, K would equal infinity, there would be no nonlinear interaction, and the amide-I energy would disperse.

In α-helical proteins the three spines are coupled to each other by additional transverse dipole-dipole interactions. This situation can be described by three coupled nonlinear Schrödinger equations. The solutions to these equations yield two types of solitons, a symmetric one in which the energy of the amide-I excitation is shared equally by all three chains and an antisymmetric one in which the amide-I energy and the accompanying deformation are shared unequally and the molecule bends (Fig. 8). The antisymmetric soliton is lower in energy and is therefore more likely to occur.

This collective excitation is called a soliton because it behaves in many ways like a particle. For example, its energy is the sum of its internal energy plus its kinetic energy, $1/2\ M_{\text{eff}}\ v^2$, where M_{eff} is the effective mass of the soliton and v is the velocity with which the excitation and accompanying distortion travel down the length of the helix. This velocity is less than the velocity of longitudinal sound in the molecule. The soliton travels with little or no energy loss and is therefore a very efficient means of energy transport along the length of the helix. Moreover, as will be shown in the mathematical development below, the soliton has an energy less than the energy of the amide-I vibration alone. It is therefore energetically favorable for solitons to form from amide-I excitations.

The mathematical model first developed by Davydov is a semiclassical approximation in which the amide-I excitations are treated quantum mechanically, and the displacements of the peptide groups, or longitudinal sound wave, along the hydrogen-bonded chain are treated classically. We will present the Davydov model for collective excitations along a single chain of hydrogen-bonded peptide groups

and show how the continuum approximation of this model leads to the nonlinear Schrödinger equation and its well-known soliton solutions. (The reader unfamiliar with the formalism of quantum mechanics may skip the next section without losing the main points of the article.)

The Davydov Model: How It Yields Soliton Solutions

The energy operator H, or Hamiltonian, for the collective excitation along the chain is a sum of three operators: $H = H_{\text{amide-I}} + H_{\text{phonon}} + H_{\text{interaction}}$, where $H_{\text{amide-I}}$ is the operator for the amide-I vibrational excitations, H_{phonon} is the operator for the displacements of the peptide groups, and $H_{\text{interaction}}$ is the operator for the interaction between the amide-I excitations and the displacements.

If E is the amide-I excitation energy and $B_n^\dagger$ is an operator for creation of this excitation on the nth peptide group, then $H_{\text{amide-I}}$ is given by

$$H_{\text{amide-I}} = \sum_n \left[EB_n^\dagger B_n - J(B_n^\dagger B_{n-1} + B_n^\dagger B_{n+1}) \right] , \qquad (1)$$

where the summation is carried out over all N peptide groups. The first term, $EB_n^\dagger B_n$, defines the amide-I excitation energy, and the second term describes the resonance dipole interaction between nearest neighbors. The operators $B_n^\dagger B_{n-1}$ and $B_n^\dagger B_{n+1}$ represent transfer of amide-I energy from peptide group n to $n \pm 1$ due to the dipole-dipole interaction. The dipole-dipole interaction energy J is given by $2|\vec{d}|^2/R^3$, which is the usual electrostatic energy associated with two colinear dipoles of moment $\vec{d}$ separated by the distance R.

The energy H_{phonon} associated with displacing the peptide groups away from their equilibrium positions is given in the harmonic approximation by

$$H_{\text{phonon}} = \frac{m}{2} \sum_n \left(\frac{du_n}{dt} \right)^2 + \frac{K}{2} \sum_n (u_n - u_{n+1})^2 , \qquad (2)$$

where u_n is the displacement of the nth peptide group, m is the mass of the peptide group, and K is the spring constant, or elasticity coefficient, of the hydrogen bonds forming the linear chain. The first term is kinetic energy and the second potential energy.

The Hamiltonian for the interaction between the amide-I excitation and the displacements of the peptide groups takes the form

$$H_{\text{interaction}} = \chi \sum_n (u_{n+1} - u_{n-1}) B_n^\dagger B_n , \qquad (3)$$

where the coupling constant χ, as mentioned earlier, represents the change in amide-I energy per unit extension of an adjacent hydrogen bond.

The total Hamiltonian $H = H_{\text{amide-I}} + H_{\text{phonon}} + H_{\text{interaction}}$ of the system must satisfy the Schrödinger equation:

$$i\hbar \frac{\partial}{\partial t} |\psi\rangle = H|\psi\rangle \quad . \qquad (4)$$

The wavefunction $|\psi\rangle$, which defines the state of the system, is expressed by

$$|\psi(t)\rangle = \sum_n a_n(t) B_n^\dagger |0\rangle \qquad (5)$$

and satisfies the normalization condition

$$\langle\psi|\psi\rangle = \sum_n |a_n(t)|^2 = 1 . \qquad (6)$$

The quantity $|a_n(t)|^2$ is the probability of finding the excitation on the nth peptide group at time t. The state $|0\rangle$ represents an unexcited amide-I vibration, that is, the ground state of the system.

Substituting Eq. 5 in Eq. 4 we get, after some algebra, the following set of differential equations:

$$i\hbar \frac{da_n}{dt} = [E + H_{\text{phonon}} + \chi(u_{n+1} - u_{n-1})] a_n - J(a_{n-1} + a_{n+1}) , \qquad (7)$$

and

$$m \frac{d^2 u_n}{dt^2} - K(u_{n+1} - 2u_n + u_{n-1}) = \chi(|a_{n+1}|^2 - |a_{n-1}|^2) . \qquad (8)$$

Equations 7 and 8 are the main result of Davydov's original model. They describe the time evolution of amide-I vibrational energy coupled to displacements of the hydrogen-bonded chain of peptide groups. The quantity $|a_n(t)|^2$ characterizes the distribution of the amide-I energy over the individual peptide groups of the chain.

In order to demonstrate that $a_n(t)$, the probability amplitude of the excitation, does behave like a soliton, we will restrict ourselves to solutions of Eqs. 7 and 8 that vary slowly as a function of the peptide group number n. In this limit we can replace the functions $a_n(t)$ and $u_n(t)$ with continuous functions $a(x,t)$ and $u(x,t)$, thus approximating n with the dimensionless coordinate x. Equations 7 and 8 then become

$$i\hbar \frac{\partial a}{\partial t} = \left(E_0 + 2\chi \frac{\partial u}{\partial x}\right) a - J \frac{\partial^2 a}{\partial x^2} \tag{9}$$

and

$$\frac{\partial^2 u}{\partial t^2} - \frac{K}{m} \frac{\partial^2 u}{\partial x^2} = \frac{2\chi}{m} \frac{\partial (|a|^2)}{\partial x} , \tag{10}$$

where

$$E_0 = E - 2J + 1/2 \int_{-\infty}^{\infty} m \left(\frac{\partial u}{\partial t}\right)^2 + K \left(\frac{\partial u}{\partial x}\right)^2 dx .$$

The left side of Eq. 10 is essentially a wave equation for longitudinal sound in the system of coupled peptide groups; the sound velocity v_s is given by $v_s = R(K/m)^{1/2}$. The right side acts as a source term for generation of sound.

We shall seek traveling wave solutions of Eqs. 9 and 10 in the form of excitations that propagate along the chain with a velocity v; that is,

$$u(x,t) = u(x - vt) . \tag{11}$$

Inserting Eq. 11 in Eq. 10, we get

$$\frac{\partial u(x,t)}{\partial x} = \frac{-2\chi}{K(1 - s^2)} |a(x,t)|^2 , \tag{12}$$

where s is the ratio of the propagation velocity to the velocity of sound: $s = v/v_s < 1$.

Substituting Eq. 12 into Eq. 9, we get

$$i\hbar \frac{\partial a}{\partial t} + J \frac{\partial^2 a}{\partial x^2} - E_0 a + \kappa |a|^2 a = 0 , \tag{13}$$

where $\kappa = 4\chi^2/K(1 - s^2)$.

Equation 13 is the nonlinear Schrödinger equation, which has soliton solutions. For its general solution we refer the interested reader to "Exact Theory of Two-Dimensional Self-Focusing and One-Dimensional Self-Modulation of Waves in Nonlinear Media" by V. E. Zakharov and A. B. Shabat (*Soviet Physics JETP* 34(1972): 62-69). It is sufficient for our purpose here to look only at a stationary solution, that is, one for which $s = 0$. In this case a solution of Eq. 13 is given by

$$a(x,t) = \frac{\chi}{(2KJ)^{1/2}} \operatorname{sech} \frac{\chi^2}{KJ} (x - x_0) \exp\left[- \frac{i}{\hbar} \left(E_0 - \frac{\chi^2}{K^2 J} \right) t \right] . \tag{14}$$

The constant x_0 is the position of maximum probability of amide-I excitation along the chain, and the pulse-shaped form given by Eq. 14 falls off rapidly when one moves away from x_0 (see "What Is a Soliton?"). Equation 14 also satisfies the continuous equivalent of Eq. 6:

$$\int_{-\infty}^{\infty} |a|^2 dx = 1 ,$$

indicating that one quantum of amide-I energy is excited on the peptide chain.

The energy E_{sol} associated with the soliton is given by

$$E_{sol} = E_0 - \frac{\chi^4}{K^2 J} \tag{15}$$

$$= E - 2J + 1/2 \int_{-\infty}^{\infty} m \left(\frac{\partial u}{\partial t}\right)^2 + K \left(\frac{\partial u}{\partial x}\right)^2 dx - \frac{\chi^4}{K^2 J} .$$

Inserting the solution given by Eq. 14, we get

$$E_{sol} = E - 2J - \frac{\chi^4}{3K^2 J} . \tag{16}$$

This is the energy of a stationary soliton. A similar but more complicated expression can be obtained for moving solitons.

It is instructive to see what happens in an absolutely rigid chain of peptide groups. In such a case $K = \infty$, and the multiplicative constant κ in the nonlinear term of Eq. 13 is equal to zero. Equation 13 is then a linear Schrödinger equation, which has solutions in the form of plane waves. This means that an excitation is uniformly distributed along the whole chain. In other words, the amide-I energy has dispersed and is no longer localized. It can also be seen from Eq. 16 that the energy of such an extended excitation (or exciton) equals $E - 2J$, which is larger by an amount $\chi^4/3K^2J$ than the energy E_{sol} of the spatially localized soliton excitation. It is thus more favorable for the system to localize its energy when the nonlinear coupling between amide-I energy and displacement of the associated peptide group is taken into account.

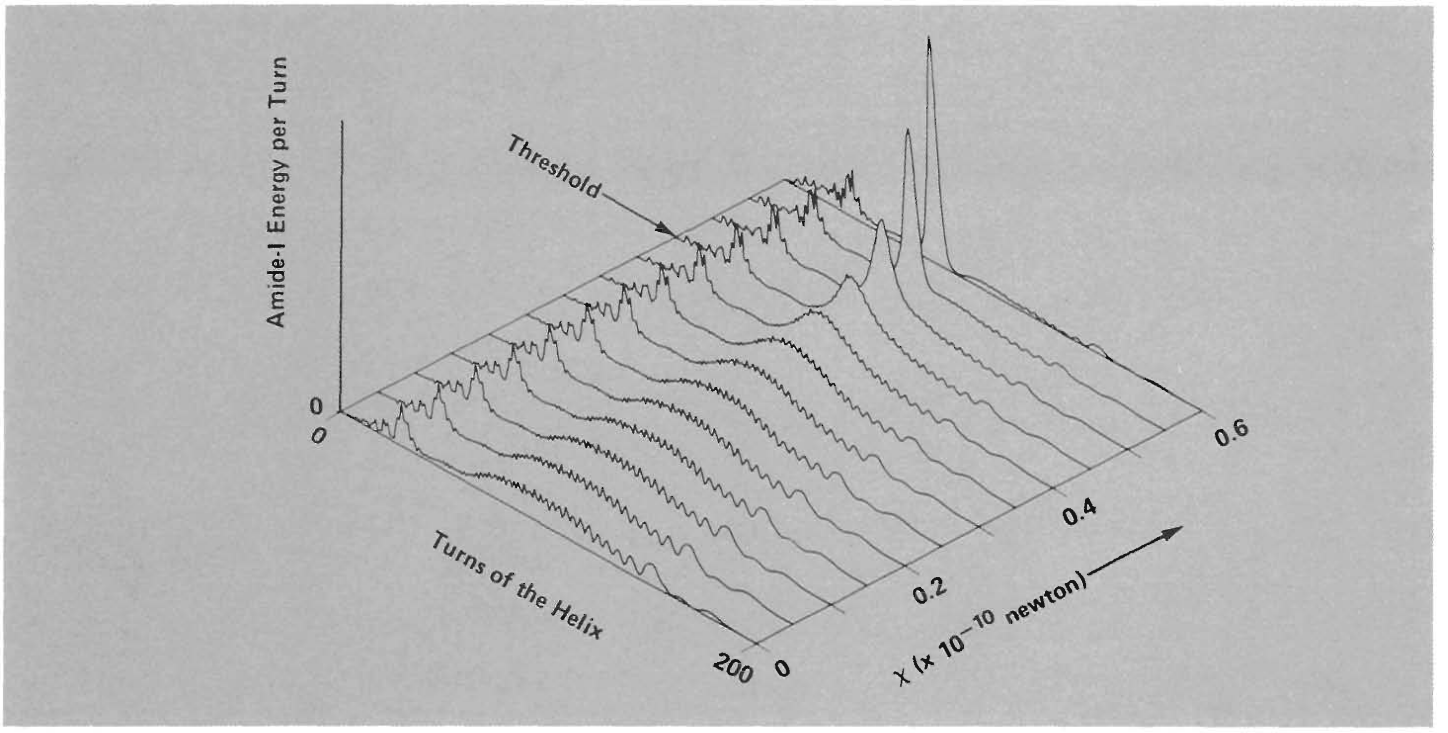

Fig. 9. Distribution of total amide-I energy (sum over all three spines) along the spines as a function of the nonlinear coupling parameter χ, as calculated numerically by L. MacNeil and A. Scott. For $\chi \geq 0.45 \times 10^{-10}$ newton, the amide-I energy self-focuses into a soliton-like excitation.

Threshold Conditions for Soliton Formation

Although the Davydov model leads to the nonlinear Schrödinger equation and soliton solutions, one can, with some justification, ask whether the nonlinear Schrödinger equation has anything to do with energy transport in a real biological system. We certainly do not expect that the smooth mathematical properties of the soliton will carry over unaltered to a real system. We do suggest, however, that the nonlinear interactions between amide-I excitations and lattice distortions will lead to stable pulse-like excitations of focused energy. Without being too dogmatic, we often find it helpful to refer to such excitations as solitons, and it is in this sense that the nonlinear Schrödinger equation serves as a useful tool in the analysis.

The strength of the coupling between amide-I vibration and lattice distortion depends on the nonlinear parameter χ. The value of this coupling constant is therefore very important when Davydov's theory is applied to real systems. In 1979 J. M. Hyman, D. W. McLaughlin, and A. C. Scott started a numerical investigation of the Davydov model applied to an α-helical protein. The equations describing this system consist of three sets of equations like Eqs. 7 and 8 but with additional terms to account for transverse dipole-dipole coupling between the three hydrogen-bonded chains of the α helix. Numerical solution of these equations yielded an important result: *The coupling between amide-I vibration and lattice distortion must be sufficiently strong for self-focusing to take place.* Below a certain threshold value a soliton cannot form and the dynamics is essentially linear. The result of a subsequent detailed investigation is summarized in Fig. 9, which shows the distribution of amide-I energy along the helix for different values of χ. For $\chi \geq 0.45 \times 10^{-10}$ newton, a soliton-like object is seen to form.

About the same time that this numerical work was being conducted at Los Alamos, an independent research effort was taking place at the Institute of Theoretical Physics in Kiev. To estimate χ from first principles, V. A. Kuprievich and Z. G. Kudritskaya were doing *ab initio* quantum-chemical calculations on the electronic structure of a dimer of formamide. This molecule consists of two peptide groups connected by a hydrogen bond and therefore serves as a tractable model for more complex protein structures. Since χ is related to the change in the C=O spring constant (K) per unit change of the hydrogen-bond length, estimates of χ can be obtained from two values of K corresponding to two hydrogen-bond lengths. Kuprievich and Kudritskaya thus estimated χ to lie between 0.3×10^{-10} and 0.5×10^{-10} newton. Careri has made an empirical estimate of χ from a comparison of amide-I energies and hydrogen-bond lengths for various polypeptide crystals. He found χ to be about 0.62×10^{-10} newton. These estimates for χ indicate that the level of nonlinearity in real systems is sufficient to allow self-focusing (soliton-like) excitations to form.

Low-Energy Spectrum of Solitons on the α Helix

Numerical studies of Davydov's model for the helix show that the collective excitations behave very much like the solitons of the nonlinear Schrödinger equation. For example, they are remarkably stable upon collision. This property is illustrated in Fig. 10, which shows the total amide-I energy (the sum over all three chains of the helix) as a function of time and peptide group number. Two solitons are launched, one from each end of the helix, by exciting two peptide groups on opposite ends of one of the three chains. The two solitons propagate in opposite directions at approximately three-eighths of the sound speed, or 17 angstroms per picosecond. They collide but pass through each other and retain their identities after the collision.

There is an internal dynamics associated with the soliton propaga-

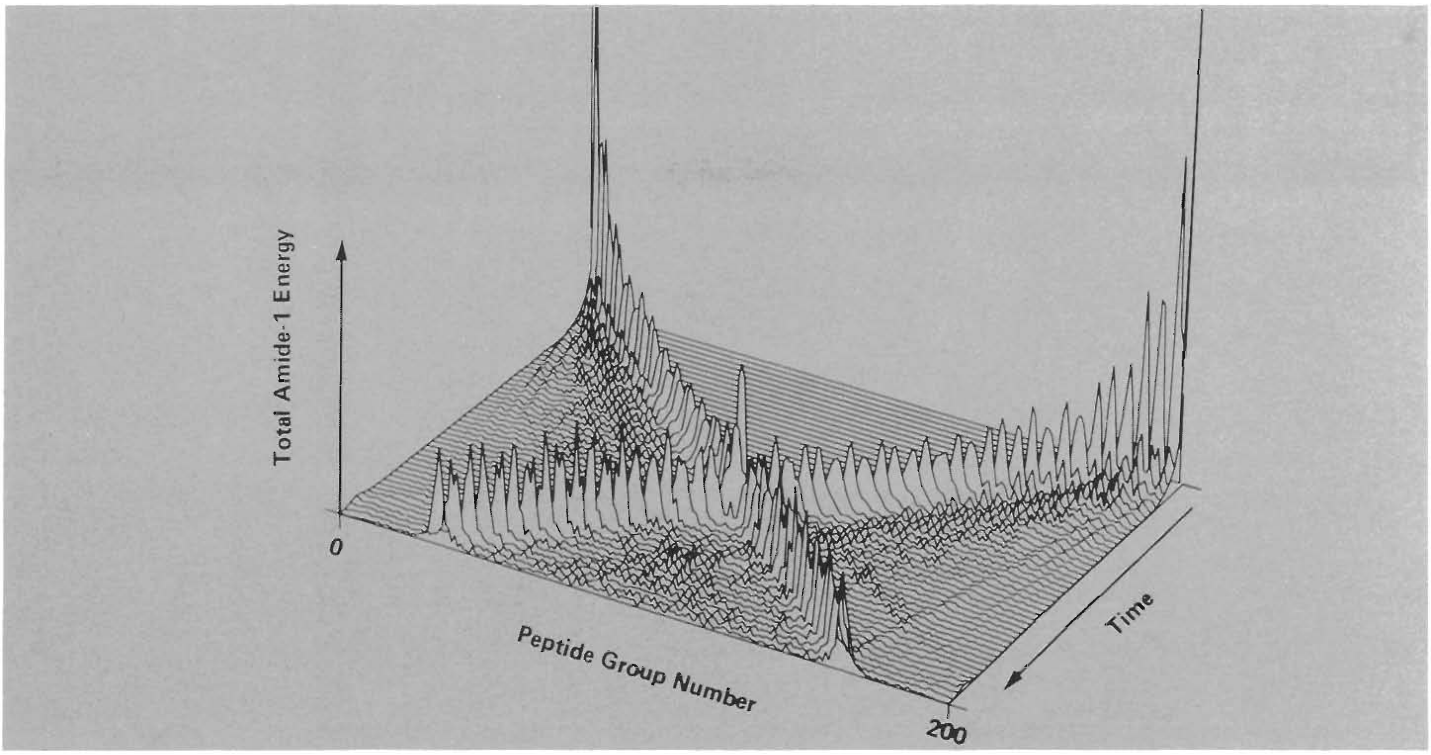

Fig. 10. Numerical calculation showing the particle-like behavior of solitons under collision. The total amide-I energy is plotted as a function of peptide group number and time. The solitons, propagating at three-eighths of the sound speed (17 angstroms per picosecond), pass through each other and maintain their identities.

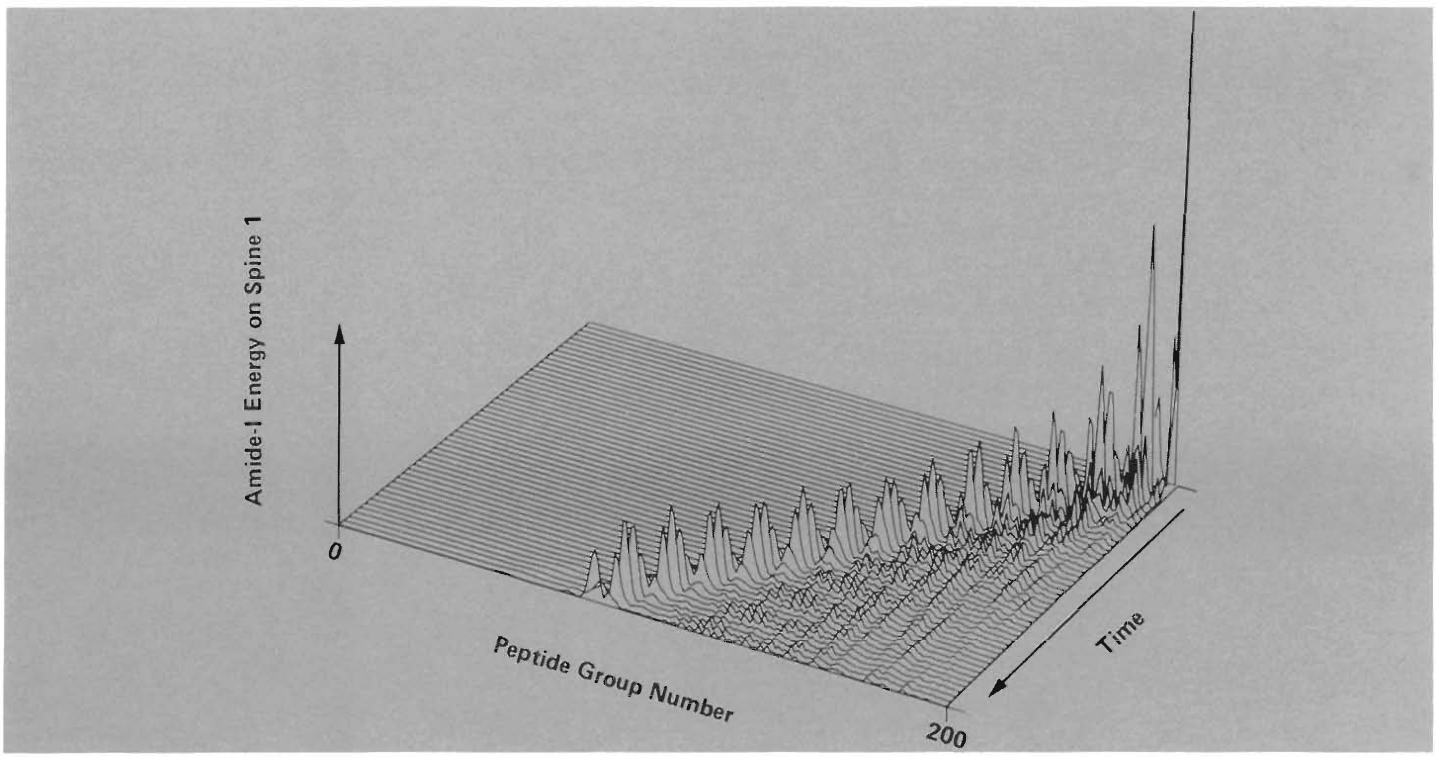

Fig. 11. Amide-I energy of spine 1 of the α helix as a function of time for a propagating soliton launched from the right end of the helix. When the energy is low on the spine shown, it is higher on the other two. The interspine oscillation of energy is caused by transverse dipole-dipole interactions among spines.

tion that cannot be appreciated from Fig. 10, namely the oscillation of soliton energy among the three spines as the soliton propagates down the length of the helix. This interspine oscillation, which is mediated by transverse dipole-dipole interactions between peptide groups on different spines, has a period of about 2 picoseconds. In Fig. 11 we show this phenomenon by depicting the amide-I energy resident on

only *one* spine. When the energy is low on the spine shown, it is higher on the other two.

The internal frequencies associated with the dynamics of a propagating soliton are in a range where many proteins are known to exhibit rich dynamic behavior. The "flutter" associated with the movement of the soliton past the periodic structure of unit cells has a spectral frequency of approximately 125 cm^{-1}, and the interspine oscillation has a frequency of approximately 20 cm^{-1}. It is therefore of interest to understand what the Davydov model for an α helix predicts in terms of the low-frequency spectrum. For this purpose we calculated the "total" bending on one spine as a function of time. The bending is defined as $u_{\alpha,1} - u_{\alpha,N}$, where α is the index of one of the three spines, and 1 and N are the numbers of the first and last groups in the chain. This quantity is shown in Fig. 12a as a function of time for two values of the coupling constant χ, one above threshold (A) and one below (B). The spectrum obtained as the square of the Fourier transform of this signal is shown in Fig. 12b. We have identified the interspine oscillation as line 1. Harmonics of this basic oscillation appear as lines 2, 3, 4, and 5. The "flutter" frequency is seen as line 7, and lines 6, 8, and 10 are interpreted as the convolution of lines 1, 2, and 3 with line 7. The lines marked A and B are subharmonics of line 1 generated through the nonlinear interaction of amide-I energy with lattice distortion. This calculated spectrum shows features that correlate well with low-frequency (below 200 cm^{-1}) spectra of metabolically active cells measured by laser Raman spectroscopy. Even though the living system is immensely more complicated than what can possibly be described within the limitations of the Davydov model, the correlation is striking enough to warrant further study.

Evidence for Solitons from a "Model Protein"

The most convincing experimental evidence for the existence of solitons in proteins comes not from the spectra of proteins or living cells but from the spectrum of the crystalline polymer acetanilide ($(CH_3CONHC_6H_5)_x$), or ACN. ACN is organized into hydrogen-bonded chains (Fig. 13) that are held together transversely by Van der Waals forces. ACN was used as an analgesic in the nineteenth century (its modern chemical cousin is Tylenol), but its interest for our purposes is its remarkable similarity to the chain structure of hydrogen-bonded peptide groups in α-helical proteins (compare Figs. 13 and 6). Late in the 1960s Careri noted that the peptide bond lengths and angles in ACN are very close to those in natural proteins, and he began an experimental program at the University of Rome to see whether ACN would show any unexpected physical properties that might be of biological interest. His intuition was rewarded in 1973 by the observation of an anomalous line in the infrared absorption spectrum of ACN. This anomalous line is lower in wave number than the main amide-I peak by 15 cm^{-1}. Its intensity is low at

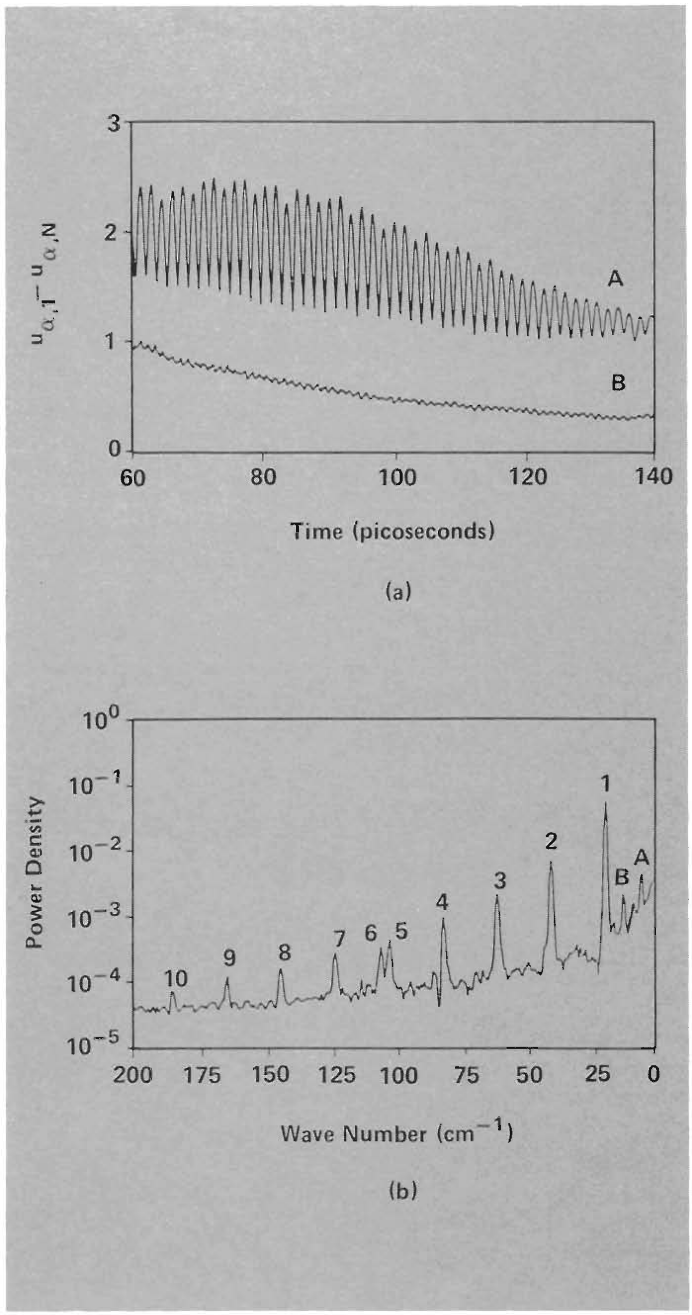

Fig. 12. (a) Time dependence of the bending of a single spine ($u_{\alpha,1} - u_{\alpha,N}$) caused by a propagating soliton for two values of χ, one above the threshold for soliton formation (A) and one below the threshold (B). (b) The spectrum obtained as the square of the Fourier transform of curve A. See the text for an interpretation of this low-frequency spectrum.

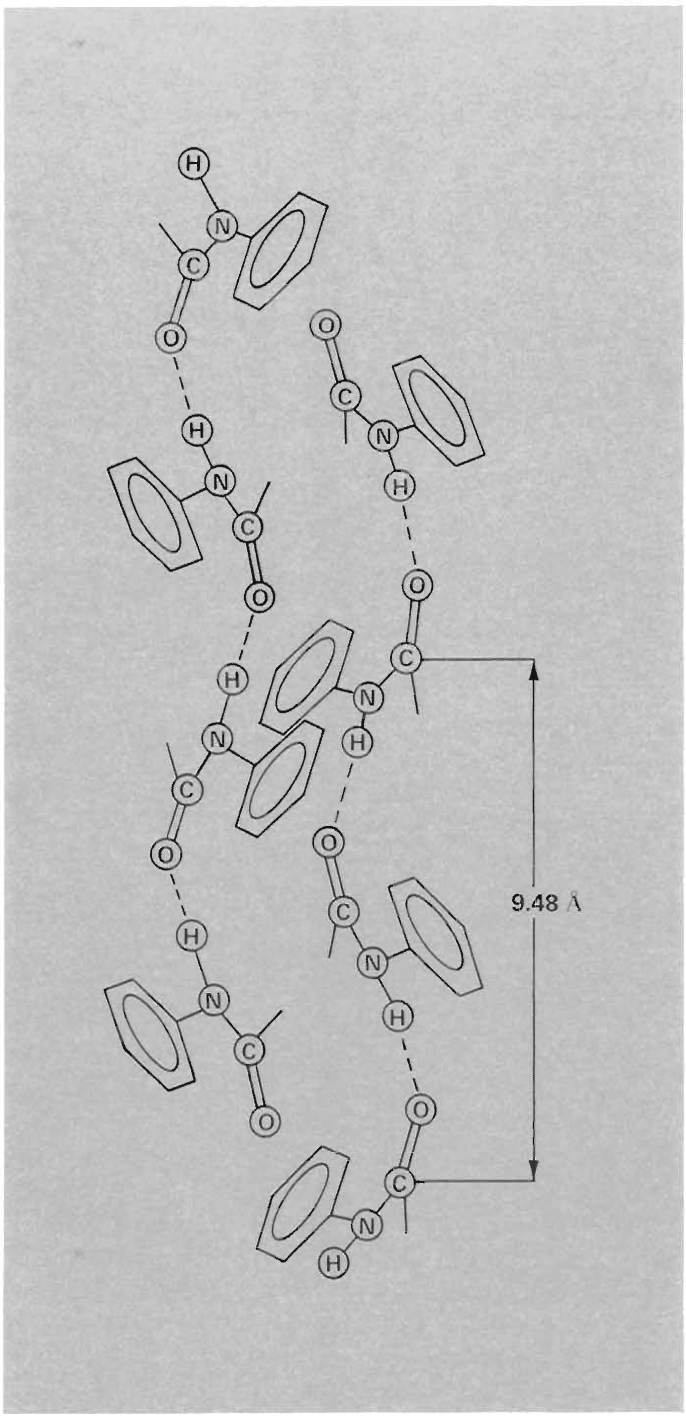

Fig. 13. A portion of two unit cells of crystalline acetanilide (ACN). The two hydrogen-bonded peptide chains resemble the spines of the α-helix shown in Fig. 6.

room temperature but increases as the temperature is lowered (Fig. 14). Numerous attempts by Careri and coworkers to find a conventional assignment for this new line were unsuccessful throughout the 1970s.

Then in 1982, when Scott became aware of Careri's data, he and Careri's group proposed that the anomalous line was due to a new type of soliton, one that results from the coupling of the amide-I vibration to an out-of-plane displacement of the hydrogen-bonding proton rather than to an in-plane displacement of the whole amide group. The soliton arising from this coupling to the lesser mass of the proton can be excited directly by electromagnetic radiation, a necessary ingredient for explaining the ACN data. The types of solitons discussed by Davydov could not be excited directly by radiation because the heavy peptide groups move too slowly about their equilibrium positions.

The mathematics of the modified theory is quite similar to the original Davydov model, and an expression similar to Eq. 16 can also be derived for the energy of this new type of soliton. Using the measured red shift of 15 cm^{-1} in this expression, Scott obtained a value for the nonlinear coupling parameter that agrees reasonably well with the estimated values of the related parameter χ.

The high-resolution ACN data of E. Gratton in Fig. 14 show the temperature dependence of the amide-I band and the anomalous band at 1650 cm^{-1}. The shoulders on the amide-I band are due to the different normal modes of amide-I excitation in the complicated unit cell of ACN. This unit cell has eight distinguishable peptide groups. The splitting of the amide-I band can thus be explained by normal-mode analysis based on group theory. The appearance of the band at 1650 cm^{-1} is consistent with the modified Davydov model and therefore may be due to the presence of solitons.

Laser Raman Spectroscopy. To further check this prediction we have repeated some of the spectroscopic measurements of Careri and coworkers and are now doing additional measurements on single crystals of ACN. (Figure 15 illustrates the principles of Raman scattering, and Fig. 16 shows the experimental setup.) Our intent is either to find alternative explanations for the 1650 cm^{-1} band or to find positive evidence for assigning it to soliton excitations.

We considered the possibility that the 1650 cm^{-1} band is due to a second-order phase transition in the crystal at low temperature. If so, the intensity of the line as a function of temperature would exhibit a threshold near some critical temperature. The measured intensity, however, shows only the smooth, gradual dependence predicted by the soliton model. Further, a second-order phase transition is expected to be accompanied by the appearance of "soft modes," which are evidenced by low-energy (less than 200 cm^{-1}) lines whose frequencies vary quadratically with temperature. No such lines were observed at temperatures ranging from 300 down to 6 kelvins.

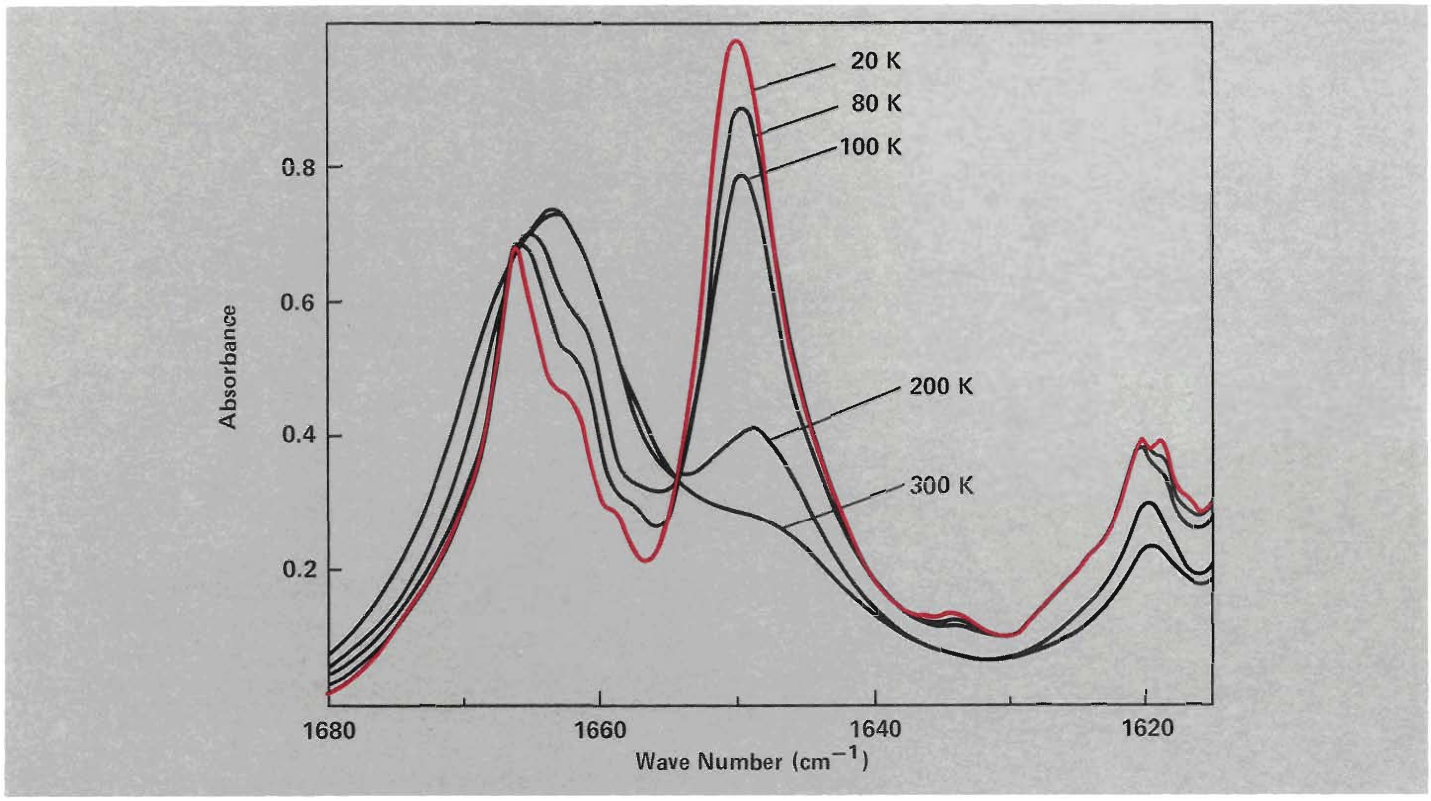

Fig. 14. Infrared spectra of ACN at different temperatures showing the amide-I band at 1665 cm^{-1} and the anomalous band at 1650 cm^{-1}. The 1650 cm^{-1} band may be caused by solitons. (Data courtesy of E. Gratton.)

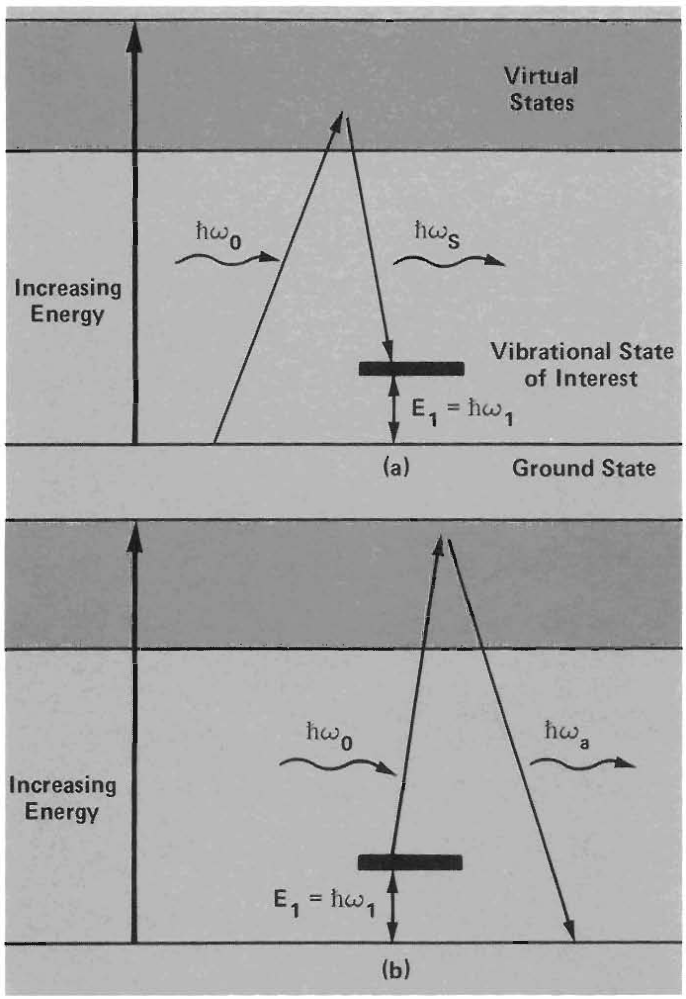

Fig. 15. Raman scattering allows one to use commonly available visible lasers and quantum detectors to analyze states whose energies correspond to wavelengths in the infrared and far-infrared spectral regions. The energy level diagrams show two types of Raman scattering, Stokes scattering (a) and anti-Stokes scattering (b). Both processes probe a particular excited state of the molecule at energy $E = \hbar\omega$. *In Stokes scattering a photon from the laser field at frequency* ω_0 *is "absorbed" by a molecule and excites it from the ground state to a "virtual state." The molecule then instantaneously decays to the state being studied (at energy level* ω_1*) and emits a photon of frequency* $\omega_S = \omega_0 - \omega_1$. *(Note that we are using the terms "frequency" and "energy" almost synonymously since they differ only by the multiplicative constant* $\hbar = h/2\pi$.*) One can think of the process as one in which the laser photon scatters off the molecule, leaving the molecule in an excited state and losing an amount of energy precisely equal to the energy of that excited state. Consequently, from the measured wavelength of the scattered photon and the known wavelength of the incident laser photon, one can determine the energy* $\hbar\omega_1$ *of the state in question, without probing it with infrared photons of frequency* ω_1. *The intensity of the Stokes line at* ω_1 *will be proportional to the population of the ground state. On the other hand, as shown in (b), some molecules may already be in the excited state. A photon of frequency* ω_0 *may raise such a molecule to a different "virtual" state from which it decays to the ground state, emitting a photon of higher frequency* $\omega_a = \omega_0 + \omega_1$. *The intensity of the anti-Stokes line at* $\omega_0 + \omega_1$ *will be proportional to the population of the excited state.*

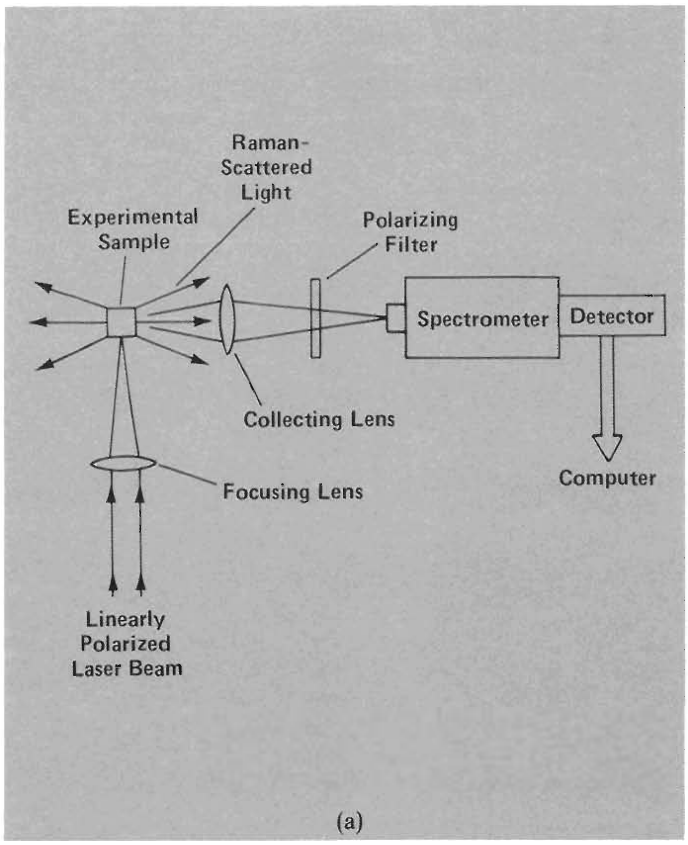

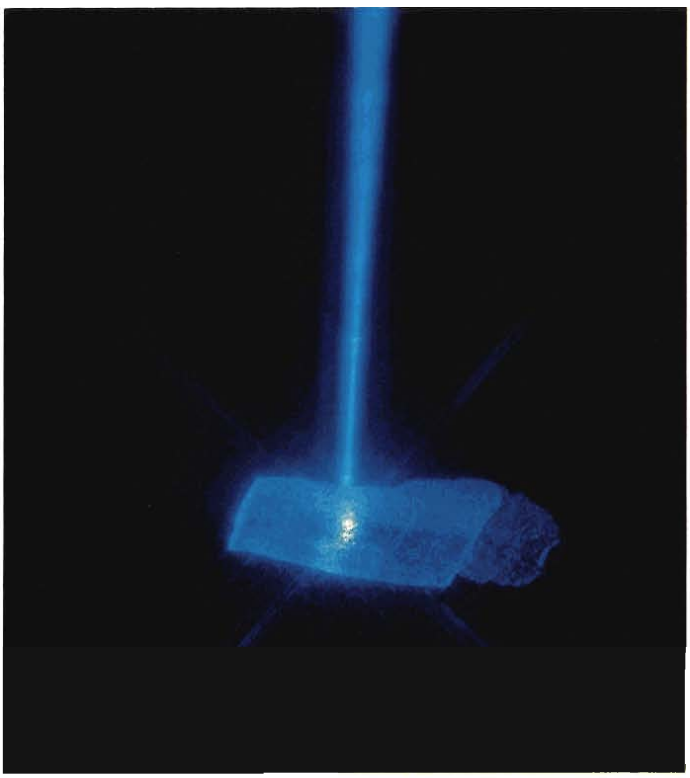

Fig. 16. (a) Experimental setup for a Raman-scattering experiment. Linearly polarized laser light is focused on a sample. Some of the scattered light is collected, usually at 90° to the incoming laser beam, by a lens or mirror. It may be passed through a polarizing filter before entering the spectrometer. (b) A single crystal of ACN scattering laser light in a laser Raman experiment at Los Alamos.

Finally, x-ray diffraction measurements of the crystal structure as a function of temperature show no evidence of structural changes.

On the positive side, if the 1650 cm^{-1} feature does correspond to a soliton, then it should mimic the behavior of the amide-I line as certain experimental parameters are varied. For example, the two lines should have the same polarization. That is, for any crystal orientation and polarization of the probing laser light, the Raman-scattered light corresponding to the line at 1650 cm^{-1} should have the same polarization as that corresponding to the 1665 cm^{-1} line. Our latest measurements (Fig. 17) show that indeed the two lines have the same polarization.

Another positive test would be to substitute carbon-13 for carbon-12 in the carbon-oxygen double bond and measure the energy shift of both lines. Almost identical energy shifts for the 1650-cm^{-1} line and the amide-I line would eliminate the possibility that the 1650-cm^{-1} line arises from some normal mode of the system other than the amide-I vibration. We are in the process of synthesizing an isotopically labeled ACN sample for this experiment.

Davydov estimated the lifetime of the soliton by taking photon-phonon interactions into account in the Hamiltonian. The radiative lifetime of the soliton is expected to be much longer than that of an exciton, or normal vibrational mode. This conjecture may also be tested with Raman spectroscopy.

To understand this, we refer to Fig. 15. In Fig. 15a it is assumed that the molecule is initially in the ground state (the most common situation), and the scattered light has a frequency $\omega_S = \omega_0 - \omega_1$. But if the molecule is initially in an excited state, then the scattering process can cause a transition down to the ground state, as shown in Fig. 15b, and the transition energy will be *added* to the laser photon, yielding a scattered photon of higher frequency $\omega_a = \omega_0 + \omega_1$. For historic reasons the former case, in which energy is lost by the light field to the molecule, is referred to as Stokes Raman scattering, whereas the latter case is called anti-Stokes Raman scattering (hence the subscripts S and a).

Since the intensity of the light scattered at frequencies ω_S and ω_a is directly proportional to the number of molecules (or population) in the ground and excited states, respectively, the ratio of anti-Stokes to Stokes scattered intensities is a direct measure of the ratio of excited to ground state populations:

$$\frac{I_a}{I_S} = \frac{P_1}{P_g} .$$

Normally (that is, under conditions of thermal equilibrium) that population ratio is given by the Boltzmann distribution formula:

$$\frac{P_1}{P_g} = \exp(-\hbar\omega_1/kT) , \qquad (17)$$

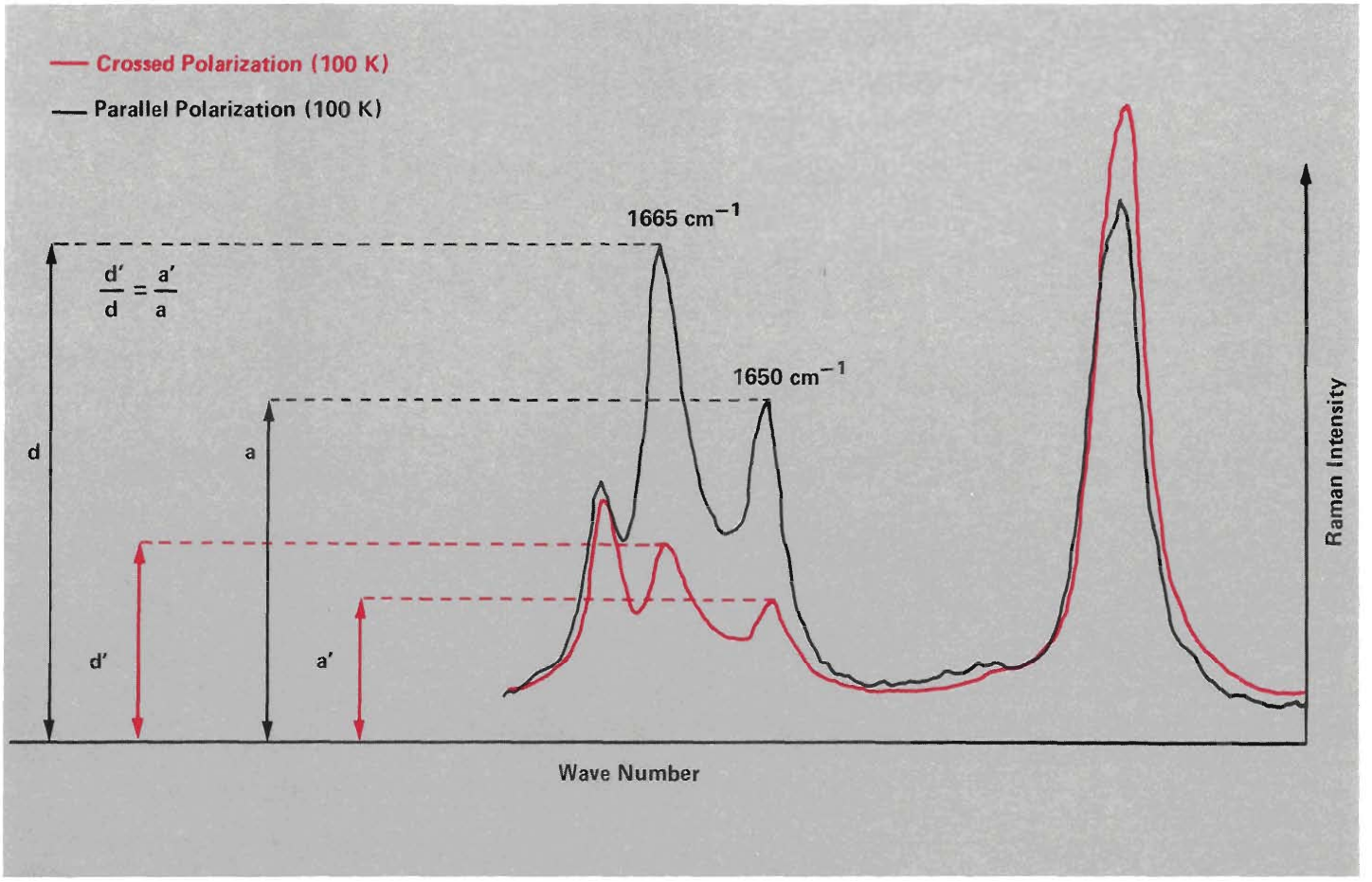

Fig. 17. Laser Raman spectra of ACN at 100 kelvins showing the 1665 cm^{-1} amide-I band and the anomalous 1650 cm^{-1} band for parallel and crossed polarizations. Since the two bands have the same ratio of parallel to crossed polarizations, they have the same polarization. This result is consistent with identification of the 1650 cm^{-1} band as a soliton arising from the self-focusing of amide-I energy.

where $\hbar\omega_1$ is the energy difference between the excited and ground states, k is the Boltzmann constant, and T is absolute temperature.

Since the soliton state is relatively stable and hence long-lived when compared with normal vibrational states of similar energy (those coupled linearly to the system), a significant excitation rate of solitons will result in a nonequilibrium, or nonthermal, population distribution. That is, the population ratio P_1/P_g will be larger than predicted by Eq. 17. Thus one would expect to see an unusually high ratio of anti-Stokes to Stokes scattering intensities when the conditions for exciting solitons exist. Those conditions could be biochemical (for example, hydrolysis of ATP) or physical (direct photoabsorption into the soliton state).

To excite the ACN soliton directly by photoabsorption, we would require a laser that emits radiation at about 1650 cm^{-1}. That wave number is available from one of the higher vibrational/rotational transitions of (what else?!) the CO molecule. We have therefore constructed a tunable electrical-discharge-excited CO laser as the excitation source. The intent is to set up a nonequilibrium population ratio by directly exciting molecules into the soliton "state." We would then expect to see unusually high anti-Stokes intensities for lines corresponding to soliton-coupled resonances.

It may also be possible to measure the lifetime of the soliton state directly. Here the techniques of ultra-fast time-resolved spectroscopy may be useful. A setup basically similar to that shown in Fig. 16 can be used but with very short-pulse excitation sources and fast detectors. The duration of the laser pulse and the temporal resolution of the detector need to be very short: between 1 and 10 picoseconds. Such measurements are being planned.

Brillouin Spectroscopy. Since the propagating soliton entails a moving density fluctuation, similar to that of a sound wave, it might be possible to scatter a photon, essentially elastically, off that fluctuation. The scattered photon would experience a Doppler shift corresponding to the speed and direction of the soliton. Then, if all the molecules of a sample were lined up, as in a crystal, all the scattered photons would experience (plus or minus) the same shift. Since the soliton speed is some fraction of the speed of sound in the crystal, corresponding to Doppler shifts between 0.01 and 0.05 cm^{-1} (300 and 1500 megahertz) the same type of equipment used to detect Brillouin (or sound wave) scattering would be applicable. This entails the use of a special type of Fabry-Perot interferometer, which is really a high-Q resonant optical cavity whose transmission is sensitive to very small changes in wavelength.

Globular Proteins

Our aim in this research is to proceed from experiments on ACN through studies of synthetic α-helical proteins to natural proteins. Although many structural proteins, such as spectrin, tropomyosin,

and myosin are almost entirely α helical, there are many other important proteins that are globular. We have seen that the competition between dispersion and focusing of amide-I energy leads—in α-helical proteins or acetanilide crystals—to the formation of a soliton-like object that can travel along the chain of hydrogen-bonded peptide groups without changing its shape. This is essentially a manifestation of the fact that the system has perfect translational symmetry. A natural question to ask is: "What is the result of the competition in globular proteins?" Such proteins do not have translational invariance among the different peptide groups, and soliton formation is not to be expected. However, the mechanisms for dispersion and focusing of amide-I energy are still present.

One way to generalize Davydov's ideas to a globular protein is to take the full geometry of the molecule into account when calculating the dipole-dipole interactions. The size of the J term in the amide-I Hamiltonian (Eq. 1) will vary from peptide group to peptide group, and all possible dipole-dipole interactions have to be considered in order to account for dispersion of amide-I energy. A preliminary computer code, based on assumptions corresponding to those leading to Eq. 13, has been developed for arbitrary protein geometry. This code provides evidence of self-focusing of amide-I vibrational energy in acetanilide (see cover) and in globular proteins. As our physical experiments evolve toward biologically realistic preparations, we plan to make corresponding improvements in this code.

Our present understanding of energy migration in biological systems is very much in its infancy. Our research efforts are directed toward identifying simple but important features in this context. The key scientific question that we have raised in this article may be stated: Is self-trapping of amide-I energy important for transport phenomena in biological materials? Experimental and theoretical studies on model proteins have so far led us to expect an affirmative answer to this question. ■

Further Reading

A. S. Davydov and N. I. Kislukha. "Solitary Excitons in One-Dimensional Molecular Chains." *physica status solidi (b)* 59(1973):465-470.

A. S. Davydov. "The Theory of Contraction of Proteins under Their Excitation." *Journal of Theoretical Biology* 38(1973):559-569.

A. S. Davydov. *Biology and Quantum Mechanics*. Oxford: Pergamon Press Ltd., 1982.

G. Careri. "Search for Cooperative Phenomena in Hydrogen-Bonded Amide Structures." In *Cooperative Phenomena*, H. Haken and M. Wagner, editors (Springer-Verlag, 1973), pp. 391-394.

V. E. Zakharov and A. B. Shabat. "Exact Theory of Two-Dimensional Self-Focusing and One-Dimensional Self-Modulation of Waves in Nonlinear Media." *Soviet Physics JETP* 34(1972):62-69.

J. M. Hyman, D. W. McLaughlin, and A. C. Scott. "On Davydov's Alpha-Helix Solitons." *Physica D* 3D(1981):23-44.

Alwyn C. Scott. "Dynamics of Davydov Solitons." *Physical Review A* 26(1982):578-595.

Alwyn C. Scott. "The Vibrational Structure of Davydov Solitons." *Physica Scripta* 25(1982):651-658.

L. MacNeil and A. C. Scott. "Launching a Davydov Soliton II: Numerical Studies." *Physica Scripta*. In press.

P. S. Lomdahl, L. MacNeil, A. C. Scott, M. E. Stoneham, and S. J. Webb. "An Assignment to Internal Soliton Vibrations of Laser-Raman Lines from Living Cells." *Physics Letters* 92A(1982):207-210.

G. Careri, U. Buontempo, F. Carta, E. Gratton, and A. C. Scott. "Infrared Absorption in Acetanilide by Solitons." *Physical Review Letters* 51(1983):304-307.

G. Careri, U. Buontempo, F. Galluzzi, A. C. Scott, E. Gratton, and E. Schyamsunder. "Spectroscopic Evidence for Davydov-Like Solitons in Acetanilide." Los Alamos National Laboratory unclassified release LA-UR-84-483 and submitted to *Physical Review B*.

Peter S. Lomdahl. "Nonlinear Dynamics of Globular Proteins." Los Alamos National Laboratory unclassified release LA-UR-83-2252 and to be published by Plenum Press in *Nonlinear Electrodynamics in Biological Systems*.

AUTHORS

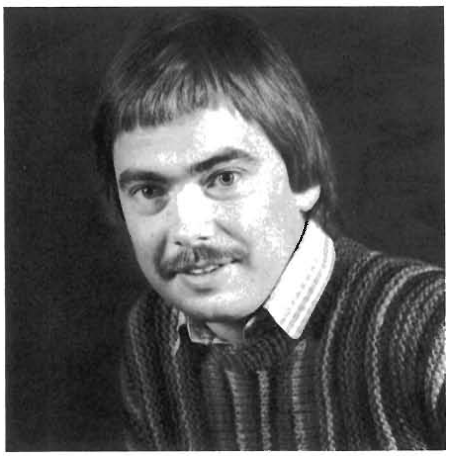

Peter S. Lomdahl was born and grew up in Copenhagen, Denmark. In 1979 he received an M.S. in electrical engineering and in 1982 a Ph.D. in mathematical physics from the Technical University of Denmark. His graduate work specialized in nonlinear wave phenomena in superconducting Josephson junctions, which is an interest he has continued after joining the Laboratory in 1982 as a postdoctoral fellow with the Center for Nonlinear Studies. The main theme in most of his research has been computer studies of nonlinear dynamics in real condensed matter materials, including conducting polymers and proteins. He has also done work on chaos and has a strong interest in numerical methods for partial differential equations.

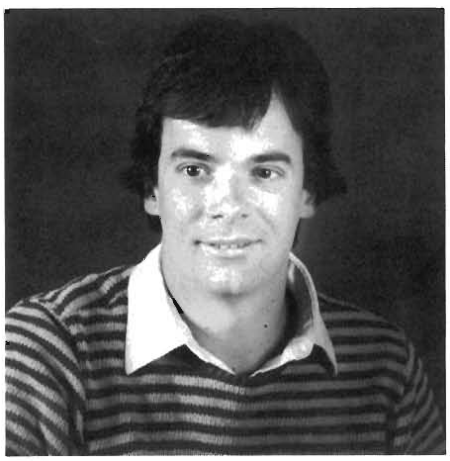

Scott P. Layne was born in Chicago, Illinois, in 1954. He received his B.A. in chemistry from DePauw University in 1976 and his M.D. from Case Western Reserve University in 1980. After completing an internship at Loma Linda University in 1981, he joined the Laboratory's Center for Nonlinear Studies as a postdoctoral fellow. Some of his interests include energy transport by biological molecules and the molecular mechanisms of general anesthesia.

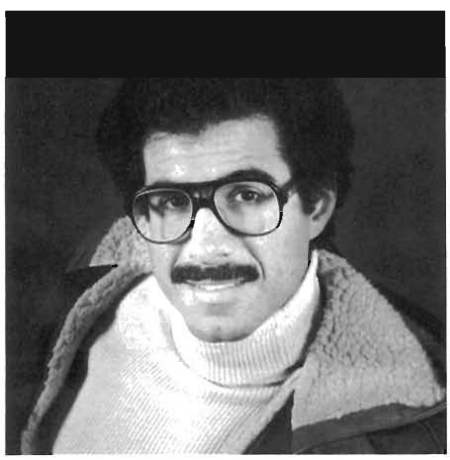

Irving J. Bigio received his B.S., M.S., and Ph.D. degrees in physics from the University of Michigan in 1969, 1970, and 1974, respectively. His doctoral work under John Ward and Peter Franken dealt with nonlinear optics, and he has maintained a broad interest in the field of quantum electronics ever since. He came directly to Los Alamos in April 1974 as a staff member in the laser isotope separation program and has also worked in the laser fusion program. In 1976 he received a Fulbright Senior Scholar Award and spent the 1976-77 academic year as a visiting professor at the Weizmann Institute of Science, Rehovot, Israel, where he taught graduate courses in laser physics and nonlinear optics and helped direct graduate student research. Since returning to Los Alamos he has resumed his research and has taught courses at the University of New Mexico Graduate Center. Currently, he is working on a variety of topics in quantum electronics and has taken an interest in the application of laser techniques and nonlinear optics to the solution of biophysics problems. He was recently appointed Deputy Leader of the Discharge Lasers Group.

A Possible Mechanism for General Anesthesia

by Scott P. Layne

RELATED TOPICS

The first general anesthesia for human surgery was administered at the Massachusetts General Hospital in Boston in 1846. The patient was put to sleep by breathing diethyl ether from a glass vesicle, and the surgeon quickly dissected a tumor located under the jaw. After completing the operation the surgeon remarked to his audience, "Gentlemen, this is no humbug."

Since this first successful demonstration of diethyl ether, researchers have discovered well over twenty drugs that induce general anesthesia. These drugs have highly diverse chemical structures and physical properties and, as a whole, lend little insight into their mechanism of action. In order to overcome this perplexity, H. Meyer and E. Overton (about the year 1900) originally proposed that anesthetic potency could be related to lipid solubility. They showed that stronger anesthetic agents were more oil-soluble than weaker ones and used this relationship to argue that anesthetics insert into the lipid bilayer and thereby expand its volume. More recent theories along this line have suggested that the expanded lipid bilayer compresses intrinsic membrane proteins and thereby disturbs normal protein shape and function. These theories have suggested also that the membrane-bound anesthetic molecules "fluidize" the lipid bilayer. This increased fluidity, in turn, alters the permeability of the membrane. While these popular ideas might be applicable to agents that are both volatile and highly lipid-soluble (oil-to-gas partition coefficient $\geq$100:1), they are not particularly suitable to a large class of *intravenous* general anesthetics that are orders of magnitude less lipid-soluble and are capable of forming hydrogen bonds. For the case of hydrogen-bonding anesthetic agents, the simplest idea is that they act by binding directly to a particularly sensitive protein, which may or may not be located in a lipid membrane, and inhibiting its normal function.

In this discussion we will focus on an important class of intravenous general anesthetics that are only slightly lipid-soluble and are capable of forming hydrogen bonds. These agents are represented primarily by *barbiturates*. From Fig. 1 it is easy to see that a barbiturate contains four H–N–C=O groups in its ring. These H–N–C=O groups are very similar to the peptide groups in proteins that are important to the propagation of solitons (see "Solitons in Biology"). The other drugs shown in Fig. 1 also contain H–N–C=O groups but to a lesser extent than barbiturates. Hydantoins contain three peptide groups, glutethimides and succinimides contain two, and urethanes contain one. These drugs are not used as general anesthetics per se, but they nevertheless have a similar inhibitory effect on the central nervous system. The potency of these six drugs appears to be related directly to the number of H–N–C=O groups in the molecule. This is supported by the fact that N-methylated barbiturates (which contain two H–N–C=O groups) are shorter acting and less potent than nonmethylated barbiturates and that trimethadione (which is devoid of H–N–C=O groups) is inactive until

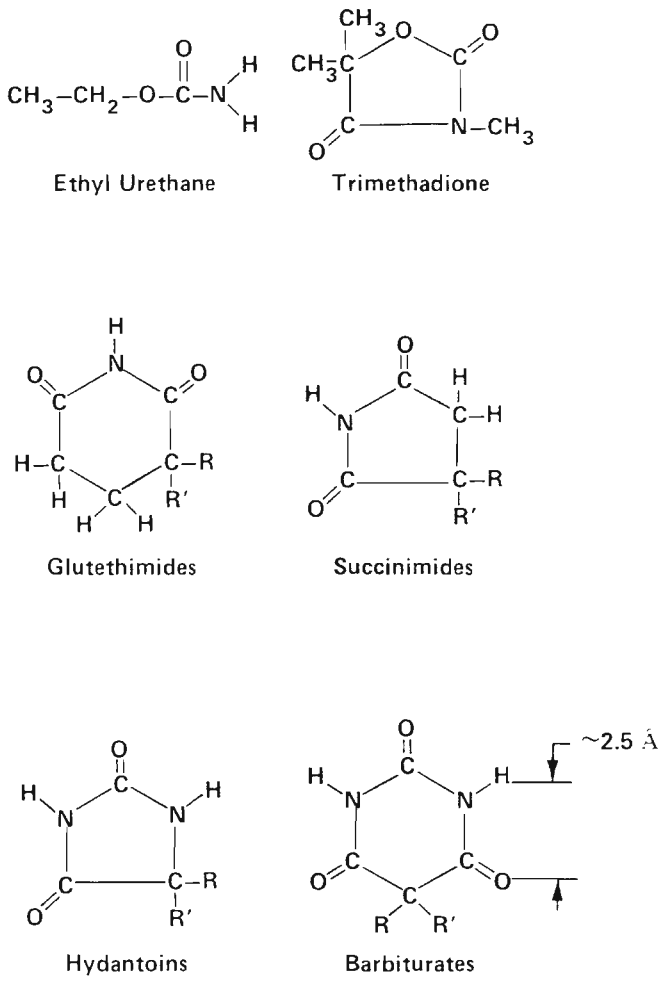

Fig. 1. The six drugs shown above, all of which contain H–N–C=O groups, inhibit the central nervous system. Hydantoins, succinimides, and trimethadione are used primarily as antiepileptic agents, whereas glutethimides are used as sedatives. Ethyl urethane is a common veterinary general anesthetic but is not used in humans because its actions are not smooth. The presence of an alkyl or aryl group at R and R′ confers increasing lipid solubility, and, generally, increased lipid solubility promotes an increased drug potency.

it is demethylated by hepatic enzymes. After demethylation, trimethadione contains two H–N–C=O groups.

C. Sandorfy and coworkers have shown by infrared spectroscopy that barbiturates are capable of dissociating hydrogen bonds in the 1-cyclohexyluracil/9-ethyladenine dimer. This dimer forms hydrogen bonds of the N–H ••• • O=C type that is common to proteins. They have also shown that barbiturates form hydrogen bonds with solutions of N,N-dimethylacetamide (NNDA) and N-methylacetamide (NMA). In this instance the N–H groups of barbiturates act as proton donors, and the O=C groups on NNDA and NMA act as proton acceptors. From these data we can infer that barbiturates are capable of forming hydrogen bonds with proteins, and, for the case of α-helical proteins, this bonding might take the form shown in Fig. 2. Note that this type of two-point hydrogen bonding along a spine of the α helix has half the chance of taking place if an N–H group in the barbiturate ring is replaced by an $N–CH_3$ group.

How does the binding of an anesthetic molecule to a protein modify normal protein behavior? We shall answer this question using the soliton model as a paradigm for *normal* protein function. The soliton model proposes that α-helical proteins effect the transport of ATP hydrolysis energy through a coupling of vibrational excitations to displacements along the spines of the helix. This coupling leads to a self-focusing of vibrational energy that has remarkably stable qualities (see "What Is a Soliton?"). We suggest that the binding of an anesthetic molecule to a protein interferes with soliton propagation. We suggest further that this type of interference would be most important in two separate regions of a cell where soliton propagation is an attractive candidate: first, in the α-helical proteins of the inner mitochondrial membrane, which appear to participate in ATP synthesis and electron transport, and second, in the membrane proteins of neurons, which are responsible for chemical reception and signal transduction. This proposal is motivated by the fact that barbiturates are capable of binding to these sites and further by the fact that these proteins have significant α-helical character. To see whether this idea makes sense from a theoretical standpoint, we need to calculate the effect of anethestic binding on soliton propagation.

When a barbiturate binds to an α helix, it will form new hydrogen bonds between anesthetic and protein molecules at the expense of the protein's hydrogen bond(s). This kind of anesthetic binding will result in either broken hydrogen bonds within the protein or in weakened hydrogen bonds of increased length; we shall call this increase ΔR. We assumed for the numerical investigation that the hydrogen bonds within the protein are merely weakened and are not completely broken. We chose for ΔR a value of 0.8 angstrom, which corresponds roughly to a decrease in hydrogen-bond energy of 55 percent. It is straightforward to calculate the new dipole-dipole interaction energy J, if we assume that the two dipoles within the protein remain colinear. The decrease in J will be proportional to $(R+\Delta R)^{-3}$. However, it is not

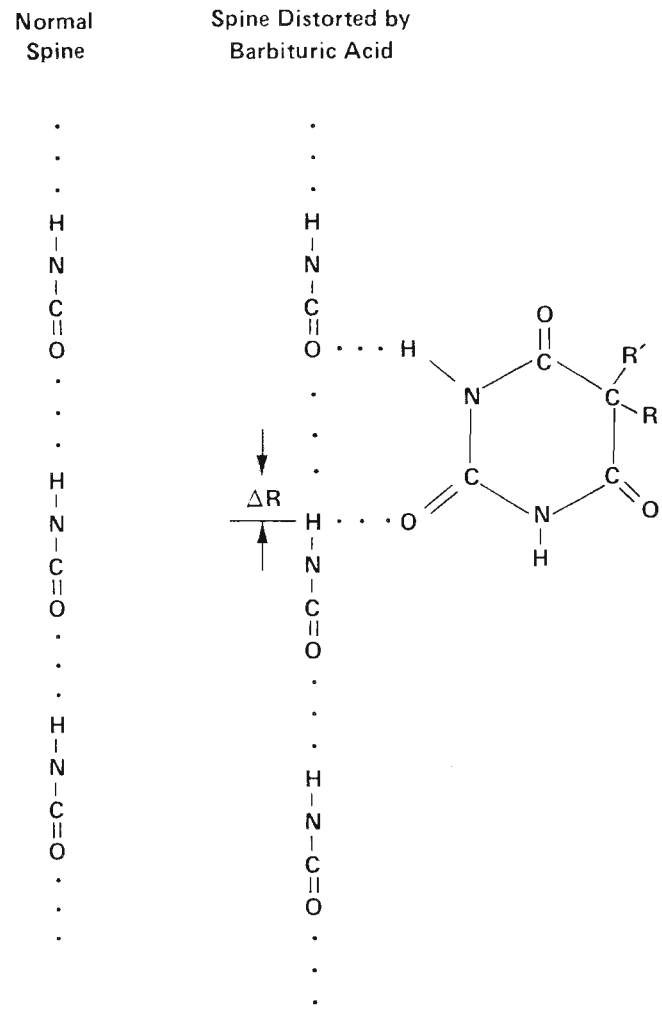

Fig. 2. A possible interaction of a barbiturate, via its H–N–C=O moieties, with one spine of an α-helical protein. The spiral configuration of the protein is stabilized by its weak hydrogen bonds, and the binding of a barbiturate changes the localized structure within the helix. In this instance, the hydrogen bond is weakened and its bond length increases by the distance ΔR.

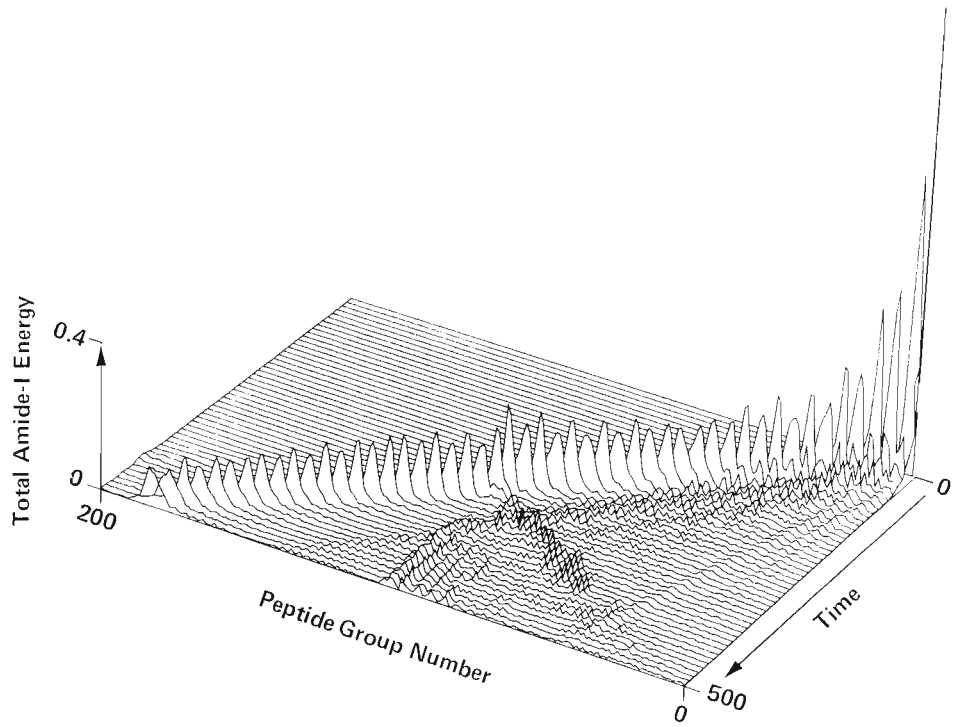

Fig. 3. Numerical calculation simulating the perturbation of a soliton by an anesthetic agent. The perturbation involves changes in the values of J, K, *and* χ *for peptide groups 100 to 103. The total amide-I energy is plotted as a function of peptide group number and time. Notice that the soliton loses amplitude and widens by the time it reaches the end of the helix.*

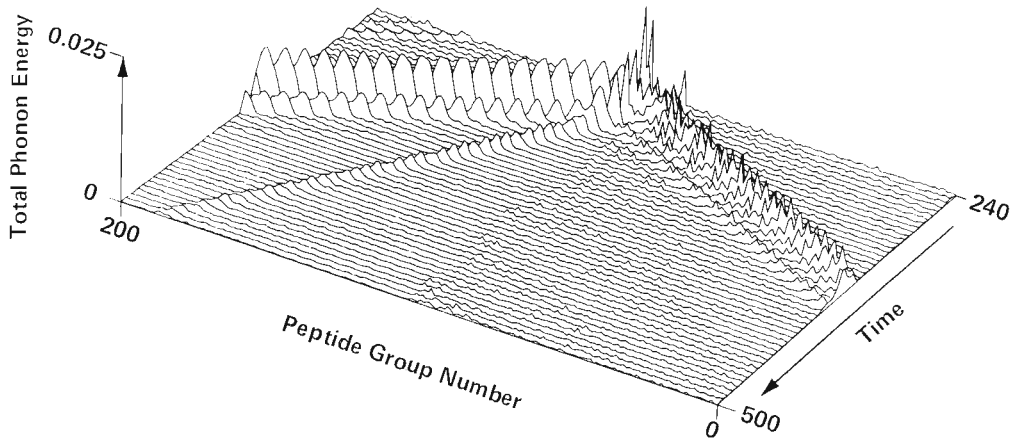

Fig. 4. This figure is the counterpart to Fig. 3. The total phonon energy is plotted as a function of peptide group number and time. In this view time has been restricted to the interval between 240 and 500 computer time units. At time 250 the soliton is just entering the region of perturbation. It radiates energy in the form of phonons as it travels through the altered peptide groups. After emerging from the region of perturbation, the soliton is seen as the low-amplitude wave, which moves at about three-eighths of the sound speed. Note that the phonon energy of the soliton is small compared to its bond energy.

as easy to calculate a new value for the hydrogen-bond spring constant K nor a new value for the coupling constant χ in weaker hydrogen bonds. As a crude estimate we assumed that K decreased proportionally to hydrogen-bond energy, and thus our new spring constant has the value of $0.45K$. We also assumed that χ is slightly decreased in weaker hydrogen bonds to the lower value that was calculated by V. Kuprievich and Z. Kudritskaya. Hence, at the point of anesthetic binding we chose $\chi = 0.3 \times 10^{-10}$ newton, which is just below threshold for soliton formation.

The results of this numerical investigation are presented in Figs. 3 and 4. The decreased values of J, K, and χ were restricted to peptide group numbers $n = 100$ to 103 on the three spines of the α helix. The perturbation was restricted to this narrow region because an anesthetic molecule is expected to weaken the hydrogen bonds in only a small region of the protein. This procedure also ensured that the soliton was well formed before entering the perturbed region. Figure 3 can be compared directly to Fig. 10 in "Solitons in Biology." It is apparent that after 500 computer time units the soliton, which traveled through the perturbation, is appreciably degraded. Figure 4 reveals that energy is radiated by the soliton in the form of phonons as it travels through the perturbation. These phonons are seen to move at the sound velocity in the α helix, which is approximately eight-thirds the soliton velocity. Up to this point we have neglected the fact that the H–N–C=O groups in the barbiturate are capable of dipole-dipole coupling to the H–N–C=O groups in the helix. Such a coupling should further degrade soliton propagation, since the interaction energy between barbiturate and α helix would be appreciable. The dipole-dipole coupling of the anesthetic molecule to the protein will depend on the number of H–N–C=O groups within it and on its spatial orientation relative to the protein.

As a final consideration of this model we pose the question: How many proteins are inhibited during general anesthesia? Barbiturates exhibit their anesthetic activity at a concentration between 200 and 1000 micromolar. At this concentration they reduce the metabolic activity of the brain by 10 to 15 percent, as measured by oxygen utilization. Taking the average membrane protein to encompass a volume of 20 angstroms × 20 angstroms × 40 angstroms = 1.6×10^4 cubic angstroms implies that about 1 percent of typical membrane proteins are associated with an anesthetic molecule. Such a small figure points out that the brain is very sensitive to alterations at the molecular level. Consciousness appears to require the coordinated effort of almost every protein.

We have presented a simplified theoretical model for anesthetic activity, taking advantage of the fact that the α helix is an important structure in membrane and cytoskeletal proteins. If the Davydov soliton finds experimental support in biology, then such a model may help to explain some of the molecular mechanisms behind general anesthesia. ■

Acknowledgment

I wish to thank Peter Lomdahl for help with the numerical code.

Further Reading

R. Buchet and C. Sandorfy. "Perturbation of the Hydrogen-Bond Equilibrium in Nucleic Bases. An Infrared Study." *Journal of Physical Chemistry* 87(1983):275-280.

N. P. Franks and W. R. Lieb. "Molecular Mechanisms of General Anaesthesia." *Nature* 300(1982):487-493.

M. Guerin, J.-M. Dumas, and C. Sandorfy. "Vibrational Spectroscopic Studies of Molecular Associations by Local Anesthetics." *Canadian Journal of Chemistry* 58(1980):2080-2088.

Scott P. Layne. "The Modification of Davydov Solitons by the Extrinsic H–N–C=O Group." Los Alamos National Laboratory unclassified release LA-UR-83-2253 and to be published by Plenum Press in *Nonlinear Electrodynamics in Biological Systems.*

RELATED TOPICS

What Is a Soliton?

by Peter S. Lomdahl

About thirty years ago a remarkable discovery was made here in Los Alamos. Enrico Fermi, John Pasta, and Stan Ulam were calculating the flow of energy in a one-dimensional lattice consisting of equal masses connected by nonlinear springs. They conjectured that energy initially put into a long-wavelength mode of the system would eventually be "thermalized," that is, be shared among all modes of the system. This conjecture was based on the expectation that the nonlinearities in the system would transfer energy into higher harmonic modes. Much to their surprise the system did not thermalize but rather exhibited energy sharing among the few lowest modes and long-time near recurrences of the initial state.

This discovery remained largely a mystery until Norman Zabusky and Martin Kruskal started to investigate the system again in the early sixties. The fact that only the lowest order (long-wavelength) modes of the discrete Fermi-Pasta-Ulam lattice were "active" led them in a continuum approximation to the study of the nonlinear partial differential equation

$$\frac{\partial u}{\partial t} + u\,\frac{\partial u}{\partial x} + \frac{\partial^3 u}{\partial x^3} = 0 \ . \qquad (1)$$

This equation (the KdV equation) had been derived in 1885 by Korteweg and de Vries to describe long-wave propagation on shallow water. But until recently its properties were not well understood.

From a detailed numerical study Zabusky and Kruskal found that stable pulse-like waves could exist in a system described by the KdV equation. A remarkable quality of these solitary waves was that they could collide with each other and yet preserve their shapes and speeds after the collision. This particle-like nature led Zabusky and Kruskal to name such waves *solitons*. The first success of the soliton concept was explaining the recurrence in the Fermi-Pasta-Ulam system. From numerical solution of the KdV equation with periodic boundary conditions (representing essentially a ring of coupled nonlinear springs), Zabusky and Kruskal made the following observations. An initial profile representing a long-wavelength excitation would "break up" into a number of solitons, which would propagate around the system with different speeds. The solitons would collide but preserve their individual shapes and speeds. At some instant all of the solitons would collide at the same point, and a near recurrence of the initial profile would occur.

This success was exciting, of course, but the soliton concept proved to have even greater impact. In fact, it stimulated very important progress in the analytic treatment of initial-value problems for nonlinear partial differential equations describing wave propagation. During the past fifteen years a rather complete mathematical description of solitons has been developed. The amount of information on nonlinear wave phenomena obtained through the fruitful collaboration of mathematicians and physicists using this description makes the soliton concept one of the most significant developments in modern mathematical physics.

The nondispersive nature of the soliton solutions to the KdV equation arises not because the effects of dispersion are absent but because they are balanced by nonlinearities in the system. The presence of both phenomena can be appreciated by considering simplified versions of the KdV equation.

Eliminating the nonlinear term $u(\partial u/\partial x)$ yields the linearized version

$$\frac{\partial u}{\partial t} + \frac{\partial^3 u}{\partial x^3} = 0 \ . \qquad (2)$$

The most elementary wave solution of this equation is the harmonic wave

$$u(x,t) = A \exp\left[i(kx + \omega t)\right] \ , \qquad (3)$$

where k is the wave number and ω is the angular frequency. In order

for the displacement $u(x,t)$ given by Eq. 3 to be a solution of Eq. 2, ω and k must satisfy the relation

$$\omega = k^3 \ . \tag{4}$$

Such a "dispersion relation" is a very handy algebraic description of a linear system since it contains all the characteristics of the original differential equation. Two important concepts connected with the dispersion relation are the phase velocity $v_p = \omega/k$ and the group velocity $v_g = \partial\omega/\partial k$. (For the dispersion relation given by Eq. 4, $v_p = k^2$ and $v_g = 3k^2$). The phase velocity measures how fast a point of constant phase is moving, while the group velocity measures how fast the energy of the wave moves. The waves described by Eq. 2 are said to be dispersive because a wave with large k will have larger phase and group velocities than a wave with small k. Therefore, a wave composed of a superposition of elementary components with different wave numbers (different values of k in Eq. 3) will disperse, or change its form, as it propagates.

Now we eliminate the dispersive term $\partial^3 u/\partial x^3$ and consider the equation

$$\partial u/\partial t + u\partial u/\partial x = 0 \ . \tag{5}$$

This simple nonlinear equation also admits wave solutions, but they are now of the form $u(x,t) = f(x - ut)$, where the function f is arbitrary. (That $f(x - ut)$ is a solution of Eq. 5 is easily verified by substitution.) For waves of this form, the important thing to note is that the velocity of a point of constant displacement u is equal to that displacement. As a result, the wave "breaks"; that is, portions of the wave undergoing greater displacements move faster than, and therefore overtake, those undergoing smaller displacements. This multivaluedness is a result of the nonlinearity and, like dispersion, leads to a change in form as the wave propagates.

A remarkable property of the KdV equation is that dispersion and nonlinearity balance each other and allow wave solutions that propagate without changing form (Fig. 1). An example of such a solution is

$$u(x,t) = 3c \ \mathrm{sech}^2[c^{1/2}(x - ct)/2] \ , \tag{6}$$

where the velocity c can take any positive value. This is the one-soliton solution of the KdV equation.

Although our discussion may have provided some glimpse of the interplay between dispersion and nonlinearity in the KdV equation, it has not, of course, provided any explanation of how solitons preserve their shapes and speeds after collision. This particle-like property is more than just a mere curiosity; it is of deep mathematical significance. A full understanding of this property requires an extensive mathematical discussion that we will not attempt here. We mention, however, that not all nonlinear partial differential equations have soliton solutions. Those that do are generic and belong to a class for which the general initial-value problem can be solved by a technique called the inverse scattering transform, a brilliant scheme developed by Kruskal and his coworkers in 1967. With this method, which can be viewed as a generalization of the Fourier transform to nonlinear equations, general solutions can be produced through a series of linear calculations. During the solution process it is possible to identify new nonlinear modes—generalized Fourier modes—that are the soliton components of the solution and, in addition, modes that are purely dispersive and therefore often called radiation. Equations that can be solved by the inverse scattering transform are said to be completely integrable.

The manifestation of balance between dispersion and nonlinearity can be quite different from system to system. Other equations thus have soliton solutions that are distinct from the bell-shaped solitons of the KdV equation. An example is the so-called nonlinear Schrödinger (NLS) equation. This equation is generic to all conservative systems that are weakly nonlinear but strongly dispersive. It describes the slow temporal and spatial evolution of the envelope of an almost monochromatic wave train. We present here a heuristic derivation of the NLS equation that shows how it is the natural equation for the evolution of a carrier-wave envelope. Consider a dispersion relation for a harmonic wave that is amplitude dependent:

$$\omega = \omega(k, |E|^2) \ . \tag{7}$$

Here $E = E(x,t)$ is the slowly varying envelope function of a modulated wave with carrier frequency ω and wave number k. The situation described by Eq. 7 occurs, for example, in nonlinear optical phenomena, where the dielectric constant of the medium depends on the intensity of the electric signal. Other examples include surface waves on deep water, electrostatic plasma waves, and bond-energy transport in proteins.

By expanding Eq. 7 in a Taylor's series about ω_0 and k_0, we obtain

$$\omega - \omega_0 = \left.\frac{\partial\omega}{\partial k}\right|_0 (k - k_0) + \frac{1}{2}\left.\frac{\partial^2\omega}{\partial k^2}\right|_0 (k - k_0)^2 + \left.\frac{\partial\omega}{\partial(|E|^2)}\right|_0 |E|^2 \ . \tag{8}$$

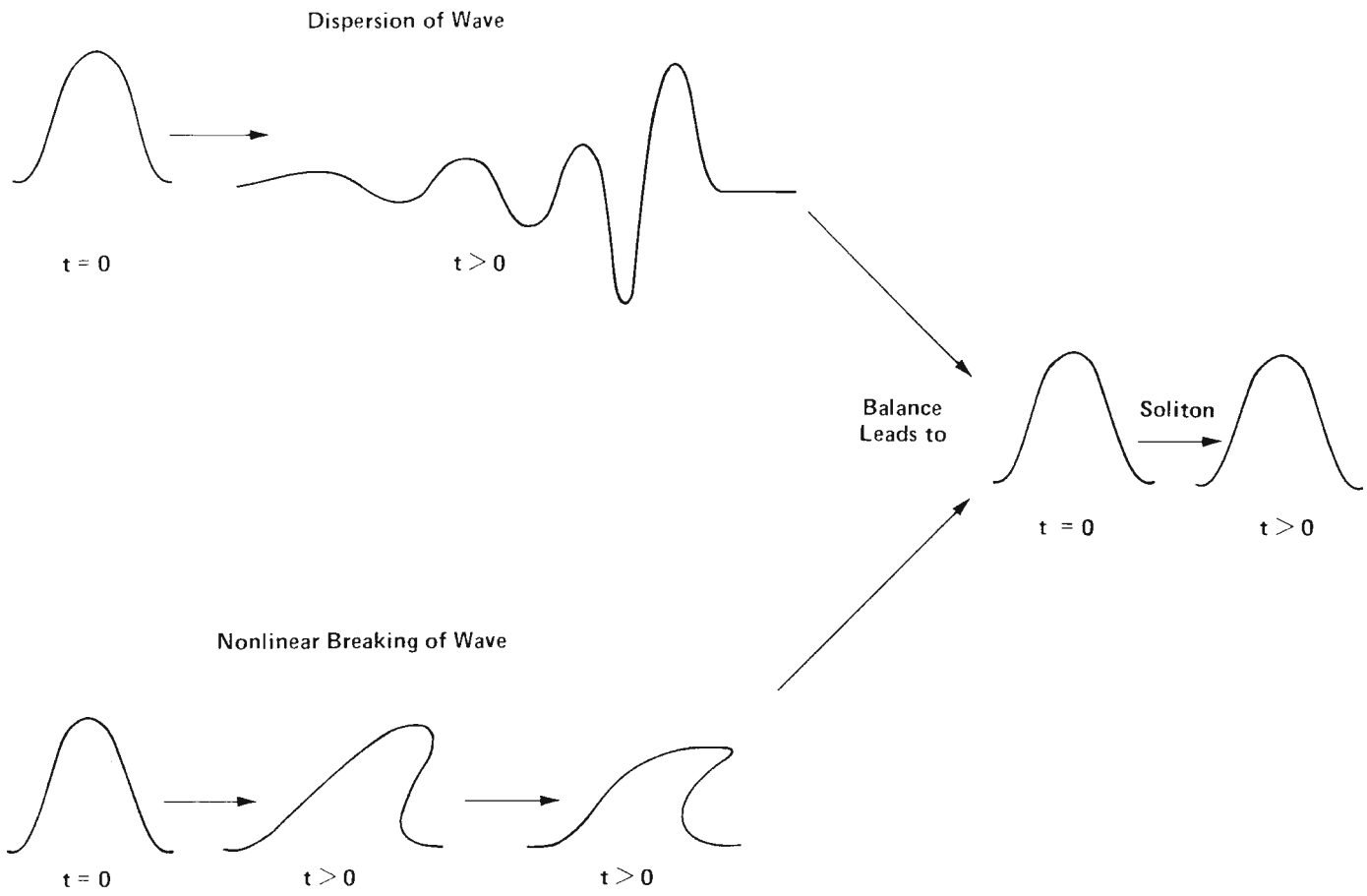

Fig. 1. Two effects, dispersion and breaking, cause the shape of a wave to change as it propagates. For a wave described by the KdV equation, these two effects balance, and the wave—a soliton—propagates without changing shape.

We have expanded only to first order in the nonlinearity but to second order in the dispersion because the first-order dispersion term, as we shall see, only represents undistorted propagation of the wave with the group velocity $v_g = [\partial\omega/\partial k]_0$. If we now substitute the operators $i(\partial/\partial t)$ for $\omega - \omega_0$ and $-i(\partial/\partial x)$ for $k - k_0$ in Eq. 8 and let the resulting expression operate on E, we get

$$i\left[\frac{\partial E}{\partial t} + \frac{\partial\omega}{\partial k}\bigg|_0 \frac{\partial E}{\partial x}\right] + \frac{1}{2}\frac{\partial^2\omega}{\partial k^2}\bigg|_0 \frac{\partial^2 E}{\partial x^2} - \frac{\partial\omega}{\partial(|E|^2)}\bigg|_0 |E|^2 E = 0 \ . \tag{9}$$

This is the nonlinear Schrödinger equation, so called because of its resemblance to the Schrödinger equation even though its derivation often has nothing to do with quantum mechanics. The first term of Eq. 9 represents undistorted propagation of the wave at the group velocity, and the second and third terms represent its linear and nonlinear distortion, respectively. This crude derivation of the NLS equation shows how it arises in systems with amplitude-dependent dispersion relations, but more formal methods are necessary if detail about the coefficients, such as $[\partial\omega/\partial(|E|^2)]_0$, is required.

It is often preferable to express Eq. 9 in a neater form. For this purpose we transform the variables x and t into z and τ, where $z = x - |\partial\omega/\partial k|_0 t$ is a coordinate moving with the group velocity and $\tau = 1/2|\partial^2\omega/\partial k^2|_0 t$ is the normalized time. Equation 9 then reduces to

$$i\frac{\partial E}{\partial \tau} + \frac{\partial^2 E}{\partial z^2} + 2\kappa|E|^2 E = 0 \ , \tag{10}$$

where

$$\kappa = -[\partial\omega/\partial(|E|^2)]_0/[\partial^2\omega/\partial k^2]_0 \ . \tag{11}$$

The NLS equation—like the KdV equation—is completely integrable and has soliton solutions. The analytic form for a single-soliton solution is given by

$$E(z,\tau) = 2\eta \ \mathrm{sech}[2\eta(\theta_0 - \eta z - 4\xi\eta\tau)] \times \exp\{-2i[\phi_0 + 2(\xi^2 - \eta^2)t + \xi z]\} \ , \tag{12}$$

where ξ, η, θ_0, and ϕ_0 are free parameters determining the speed, amplitude, initial position, and initial phase, respectively, of the soliton. Figure 2 shows the profile of this soliton.

Any initial excitation for the NLS equation will decompose into solitons and/or dispersive radiation. A monochromatic wave train solution $E(z,\tau) = E(\tau)$ is thus unstable to any z-dependent perturbation and breaks up into separate and localized solitons. This phenomenon is called the Benjamin-Feir instability and is well known to any surfer on the beach who has noticed that every, say, seventh wave is the largest. The NLS equation is in a way more universal than the KdV equation since an almost monochromatic, small-amplitude solution of the KdV equation will evolve according to the NLS equation.

The last type of soliton we mention, which is distinctly different from the KdV or NLS solitons, is one that represents topologically invariant quantities in a system. Such an invariant can be a domain wall or a dislocation in a magnetic crystal or a shift in the bond-alternation pattern in a polymer. The prototype of equations for such solitons is the sine-Gordon equation,

$$\frac{\partial^2 u}{\partial x^2} - \frac{\partial^2 u}{\partial t^2} = \sin u \ . \tag{13}$$

Notice that this equation allows for an infinite number of trivial

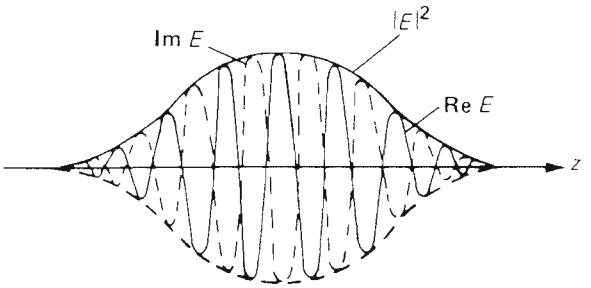

Fig. 2. Profile of a single-soliton solution of the NLS equation.

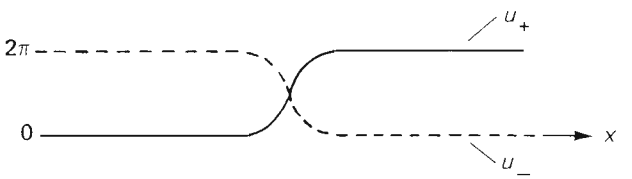

Fig. 3. Profiles of soliton solutions of the sine-Gordon equation.

RELATED TOPICS

solutions, namely $u = 0, \pm 2\pi, \pm 4\pi, \ldots$. Systems with a multitude of such "degenerate ground states" also allow solutions that connect two neighboring ground states. Solutions of this type are often called kinks, and for the sine-Gordon equation they are exact solitons; that is, they collide elastically without generation of dispersive radiation. The analytic form, whose profile is shown in Fig. 3, is given by

$$u_{\perp}(x,t) = 4 \tan^{-1}\{\exp[\pm(x - x_0 - ct)/(1 - c^2)^{1/2}]\} , \qquad (14)$$

where the solution u_{-} is often called an antikink. The parameter c $(-1 < c < 1)$ determines the velocity and x_0 the initial position. Other equations with degenerate ground states also have kink and antikink solutions, but they are not exact solitons like those of the sine-Gordon equation. It is interesting to note that small-amplitude solutions of the sine-Gordon equation also can be shown to evolve according to the NLS equation.

Equations with soliton solutions are generic, and, although real systems often contain mechanisms (impurities, dissipative forces, and multidimensionality) that destroy exact soliton behavior, they are very useful as a starting point for analysis. In fact, perturbation methods—with the perturbation taking place around the soliton—have been developed to compute the response of the soliton to external forces, damping, etc. Often the result is that the parameters characterizing the soliton (such as velocity and amplitude) are now time dependent, with the time dependence governed by simple ordinary differential equations. The original equations are therefore still very useful. Because the mechanisms that give rise to soliton equations are so prevalent, the suggestion that solitons might arise in biology is not so surprising. The question to be asked is how well a particular biological system satisfies the criteria underlying the soliton equation. ■

Further Reading

The classic paper where the word "soliton" was introduced is "Interaction of 'Solitons' in a Collisionless Plasma and the Recurrence of Initial States" by N. J. Zabusky and M. D. Kruskal in *Physical Review Letters* 15(1965):240. For many references see also "Computational Synergetics and Mathematical Innovation" by Norman J. Zabusky in *Journal of Computational Physics* 43(1981):95.

There are an increasing number of papers on solitons; a good review paper covering the subject to 1973 is "The Soliton: A New Concept in Applied Science" by Alwyn C. Scott, F. Y. F. Chu, and David W. McLaughlin in *Proceedings of the IEEE* 61(1973):1443.

Good accounts of the subject, together with up-to-date lists of references, can also be found in many textbooks, including the following.

G. L. Lamb, Jr. *Elements of Soliton Theory*. New York: John Wiley & Sons, 1980.

Mark J. Ablowitz and Harvey Segur. *Solitons and the Inverse Scattering Transform*. Philadelphia: Society for Industrial and Applied Mathematics, 1981.

R. K. Dodd, J. C. Eilbeck, J. D. Gibbon, and H. C. Morris. *Solitons and Nonlinear Wave Equations*. New York: Academic Press, 1982.